

1983

Structural studies of electroless thin Ni-P films grown in an alkaline environment.

Raul. Cortijo
University of Windsor

Follow this and additional works at: <http://scholar.uwindsor.ca/etd>

Recommended Citation

Cortijo, Raul, "Structural studies of electroless thin Ni-P films grown in an alkaline environment." (1983). *Electronic Theses and Dissertations*. Paper 3619.

This online database contains the full-text of PhD dissertations and Masters' theses of University of Windsor students from 1954 forward. These documents are made available for personal study and research purposes only, in accordance with the Canadian Copyright Act and the Creative Commons license—CC BY-NC-ND (Attribution, Non-Commercial, No Derivative Works). Under this license, works must always be attributed to the copyright holder (original author), cannot be used for any commercial purposes, and may not be altered. Any other use would require the permission of the copyright holder. Students may inquire about withdrawing their dissertation and/or thesis from this database. For additional inquiries, please contact the repository administrator via email (scholarship@uwindsor.ca) or by telephone at 519-253-3000ext. 3208.

CANADIAN THESES ON MICROFICHE

I.S.B.N.

THESES CANADIENNES SUR MICROFICHE



National Library of Canada
Collections Development Branch

Canadian Theses on
Microfiche Service

Ottawa, Canada
K1A 0N4

Bibliothèque nationale du Canada
Direction du développement des collections

Service des thèses canadiennes
sur microfiche

NOTICE

The quality of this microfiche is heavily dependent upon the quality of the original thesis submitted for microfilming. Every effort has been made to ensure the highest quality of reproduction possible.

If pages are missing, contact the university which granted the degree.

Some pages may have indistinct print especially if the original pages were typed with a poor typewriter ribbon or if the university sent us a poor photocopy.

Previously, copyrighted materials (journal articles, published tests, etc.) are not filmed.

Reproduction in full or in part of this film is governed by the Canadian Copyright Act, R.S.C. 1970, c. C-30. Please read the authorization forms which accompany this thesis.

THIS DISSERTATION
HAS BEEN MICROFILMED
EXACTLY AS RECEIVED

AVIS

La qualité de cette microfiche dépend grandement de la qualité de la thèse soumise au microfilmage. Nous avons tout fait pour assurer une qualité supérieure de reproduction.

S'il manque des pages, veuillez communiquer avec l'université qui a conféré le grade.

La qualité d'impression de certaines pages peut laisser à désirer, surtout si les pages originales ont été dactylographiées à l'aide d'un ruban usé ou si l'université nous a fait parvenir une photocopie de mauvaise qualité.

Les documents qui font déjà l'objet d'un droit d'auteur (articles de revue, examens publiés, etc.) ne sont pas microfilmés.

La reproduction, même partielle, de ce microfilm est soumise à la Loi canadienne sur le droit d'auteur, SRC 1970, c. C-30. Veuillez prendre connaissance des formules d'autorisation qui accompagnent cette thèse.

LA THÈSE A ÉTÉ
MICROFILMÉE TELLE QUE
NOUS L'AVONS REÇUE

STRUCTURAL STUDIES OF ELECTROLESS THIN Ni-P FILMS
GROWN IN AN ALKALINE ENVIRONMENT

by

Raul Cortijo

A Thesis

Submitted to the Faculty of Graduate Studies through the
Department of Physics in Partial Fulfillment of the
Requirements for the Degree of Master of Science
at the University of Windsor

Windsor, Ontario

1983

© Raul Cortijo 1983

789739

Abstract

A comparative study of the microstructure of electrolessly deposited Ni-P thin films grown from an alkaline bath with different pH values was performed. Using Radial Distribution Function (RDF) analysis of the diffraction patterns a model for the structure is given and it is concluded that the films differ mainly by the sizes of their component crystallites. The crystallites while retaining a high degree of order, exhibit a liquid like character due to their large surface to volume ratio.

Acknowledgement

I would like to express my sincere thanks to Dr. M. Schlesinger for his supervision and continual guidance in this project. I also wish to thank Dr. R. Helbing for kindly letting me use his computer facilities to get this thesis printed, to Mr. J. Robinson for his technical help in areas dealing with the electron microscope and last but not least I would like to thank my wife Melissa for providing moral support.

Table of Contents

	page
Abstract	i
Acknowledgement	ii
List of Figures	iv
List of Tables	v
Chapter I Introduction	1
Chapter II Experimental	3
Chapter III Theoretical Considerations	
I) Introduction	9
II) Atomic Elastic Scattering	
i) Classical Treatment	11
ii) The Schrodinger Equation	12
iii) Asymptotic Solution	15
III) Scattering by an Ensemble of Atoms	25
Chapter IV Data Analysis,	30
i) Non linear photographic film response	32
ii) Termination Effects	38
iii) Normalization	44
iv) Non elastic Scattering	48
Chapter V Results and Discussion	50
Appendix 1 Computer Implementation	64
Appendix 2 Program Listings	66
References	89
Vita Actoris	92

List of Figures

	page
Figure IV-1 Typical characteristic curve for photographic film	33
Figures IV-2 Series of diffraction pattern curves of the same sample taken with varying exposure time and IV-3	35
Figure IV-4 Plot of diffuse density vs. exposure time for the different well defined peaks present in figures IV-2 and IV-3	37
Figure IV-5 Square wave pulse truncating function and corresponding Fourier transform	40
Figure IV-6 Triangular truncating and corresponding Fourier transform	42
Figure IV-7 Hanning truncating and corresponding Fourier transform	43
Figure IV-8 $I(s)/N$ and $f^2(s)$ curves for typical sample	45
Figure V-1 Transmission electron micrographs of electrolytically deposited Ni-P films from an alkaline solution grown at different pH values	51
Figure V-2 Diffraction pattern curves corresponding to the films shown in figure V-1	55
Figures V-3 $i(s)$ curves obtained after the correction and V-4 procedures	55

Figures V-5, Reduced RDF $G(r)$ curves for films corresponding to (A) - (D) in figure V-2

List of Tables

	page
Table II-1 Film deposition process	4
Table II-2 Composition of sensitizer solution	5
Table II-3 Composition of activator solution	5
Table II-4 Composition of metallizing bath	5
Table II-5 Electron Microscope setting for all films examined	7
Table II-6 Diffraction pattern recording process	8
Table V-1 Island and crystallite sizes	56
Table V-2 First ten peak locations in $G(r)$ curves	61

Chapter I

Introduction

The electrolessly deposited films continue to attract a great deal of attention in both scientific and industrial fields. From an industrial point of view electroless films provide a relatively cheap method to plate non conductive materials. Using the photo-selective properties of the deposition of these films one can create negative or positive images. This fact has been widely used in the printed board industry. As a matter of fact, all PC boards in the new generation IBM computers have been electrolessly deposited⁽¹⁾. From the physicist point of view these films provide an interesting range of systems from totally amorphous to crystalline.

The present work deals with one specific electrolessly deposited thin metal system, Ni-P films grown in alkaline environment. Ni-P films grown in acidic solution have been the subject of a large amount of research work for under the proper conditions they can exhibit total amorphicity^(2,3,4). On the other hand basic grown Ni-P has not been treated until very recently. One of the newly discovered properties is that using the same basic solution both photo-selective negative and positive deposition is possible⁽⁵⁾. It is, also known that the amount of co-deposited phosphorous varies the amount of crystallinity of the films. The aim of the present work is to clarify the nature of the partial crystallinity observed.

Radial distribution functions, RDF, will be calculated for a series of films grown in metallizing baths of different pH

Chapter I: Introduction

values. It will become evident that the application of RDF techniques is a powerful means to study the micromorphology of partially crystalline materials.

This thesis is divided into four additional chapters. Chapter II deals with the experimental procedures, Chapter III is a theoretical exposition of the necessary steps involved in the calculation of RDF curves, Chapter IV takes up the data analysis and correction procedures, finally Chapter V presents the results and discussion. In addition two appendices are included. Appendix 1 describes the logic structure of the computer routines used in this work while Appendix 2 gives the actual source listing of the programs.

CHAPTER II

Experimental

1 Films

i) Deposition

The thin films used for this study were grown on microscope glass slides coated with a thin layer of Formvar. In order to apply the Formvar layer the following procedure was used. The glass slide was placed inside a large burette and Formvar solution, consisting of 4g of polyvinylformal in 1l of ethylene dichloride, was run through the burette. The thickness of the Formvar layer is directly proportional to the flow rate of the solution i.e. to obtain a thin Formvar layer the solution must be drained at a very slow rate, typically a Formvar solution of 250 ml was drained in 10 seconds.

The films were grown following standard electroless deposition techniques (6,7) (see Table II-1). The Formvar substrate was activated by immersing the slide successively in solutions of SnCl_2 and PdCl_2 . These solutions are referred to as Sensitizer and Activator respectively. Their overall effect is to form nucleation centers on which the metal films start to grow. The metallizing bath was kept at a constant temperature of 43°C and its pH was recorded with a FISHER DIGITAL pH METER 107 while the films were deposited. The slide was left in the metallizing bath until the films had grown to give a smooth metallic shine. This was an indication that the metal film was nearly continuous (see figure V-1). The time required for deposition varied as a function of the pH of the bath. The actual composition of all solutions used is given in Tables II-2 to II-4.

ii) Sample Preparation

As soon as the deposition process was finished, the slide was rinsed in distilled water, then the metallized Formvar layer was separated from the glass slide by partially floating it in distilled water. At this point an electron microscope sample holder grid was inserted between the glass and the Formvar. The water was then removed taking special care that the grid remained between the Formvar and the glass at the desired position. After the slide was nearly dry the metal film was cut around the grid, which could then be lifted by a pair of fine tweezers. The films were not dried totally because the Formvar layer would stick again to the glass and the grid would not lift from the glass slide without breaking the metallized Formvar layer sitting on the grid.

SOLUTION	TIME
Sensitizer	2.5 min
Rinse	30 sec
Activator	3 min
Rinse	30 sec
Metallizing	pH dependent

Table II-1 Film deposition process

Chapter II: Experimental

STOCK		
Stannous Chloride	$\text{SnCl}_2 \cdot \text{H}_2\text{O}$	10g
Hydrochloric acid	HCl	10ml
WORKING SOLUTION		
0.5 ml of stock solution in 160 ml H_2O		

Table II-2 Composition of Sensitizer Solution

STOCK		
Palladium Chloride	PdCl_2	10g
Hydrochloric acid	HCl	10ml
WORKING SOLUTION		
1 ml of stock solution in 200ml of H_2O		

Table II-3 Composition of Activator Solution

STOCK		
Nickel Sulfate	$\text{NiSO}_4 \cdot 6\text{H}_2\text{O}$	30g/l
Sodium Hypophosphite	$\text{NaH}_2\text{PO}_2 \cdot \text{H}_2\text{O}$	10.6g/l
Sodium Citrate	$\text{Na}_3\text{C}_6\text{H}_5\text{O}_7 \cdot 2\text{H}_2\text{O}$	200g/l
Ammonium Chloride	NH_4Cl	53.6g/l
WORKING SOLUTION		
Add concentrated NaOH to adjust pH to desired value.		

Table II-4 Composition of metallizing Solution

2 Electron Microscopy

Since a number of different samples were studied and the results were to be compared a standard examination technique was developed. The main goal was to view these samples in the "as deposited" state, thus all samples were examined the same day they were grown. It is also known that heat treatment will transform the as deposited Ni-P films to a series of different phases until a stable two phase state of face centered cubic Ni and body centered tetragonal Ni_3P is reached (8).

Hence if during the examination of the samples the electron beam is condensed to a small size it can heat the sample causing it to deteriorate by changing state. This heating technique can actually sometimes be useful and has been successfully used by other authors to study the different phases of Ni-P films (9), however in this study parameters were chosen (see Table II-5) so that the electron beam width and intensity caused no heating effects leaving the samples in the as deposited state. The electron microscope used for the examination of the samples was a JEOL model JEM-100CX. The sources of experimental data were Bright Field electron micrographs and Selected Area Diffraction patterns which were recorded photographically on KODAK Electron Image Film 4463. The effective focal length used for the SAD was calculated using a standard thin film of pure aluminum.

3 Recording of Diffraction Patterns

The photographic films with the diffraction patterns were scanned by a standard JARRELL ASH densitometer at a speed of 25 mm/min. The densitometer was equipped with a non cooled RCA IP28

Chapter II: Experimental

photomultiplier which gave a small current signal, up to 3.0×10^{-5} amps, that was fed to a KEITHLEY 410 micro-microammeter. This ammeter is provided with an output for driving a strip chart recorder, and it generates a 5 volt signal at full scale meter deflection which is particularly suitable for use as the input of a DEC ADV11-A analog to digital converter (ADC). The ADC samples an analog voltage signal in the range of -5V to 5V and converts it to a series of octal numbers from 0 to 7777. The ADC was controlled by a program implemented in a PDP 11/03 computer (see appendix 1), whose action was to determine the sampling rate, eliminate random noise and to store the data in ASCII files for later use. The elimination of the random background noise was achieved by performing two different types of averaging. First, to facilitate calculations it was desired to digitize the diffraction pattern to 1024 points, each of these points being the average of 8 consecutive sampled points. Second, many runs of each diffraction pattern were taken and the overall average determined. A diagram representing the recording process is given in Table II-6.

Accelerating voltage	100 KV
Electron micrographs	
Objective aperture	120 μ m
Magnification	20000 X
Photographic exposure	5.6 sec
Selected Area Diffraction	
Field aperture	250 μ m
Focal length	236mm
Photographic exposure	see chapter IV

Table II-5 Electron Microscope setting for all films examined

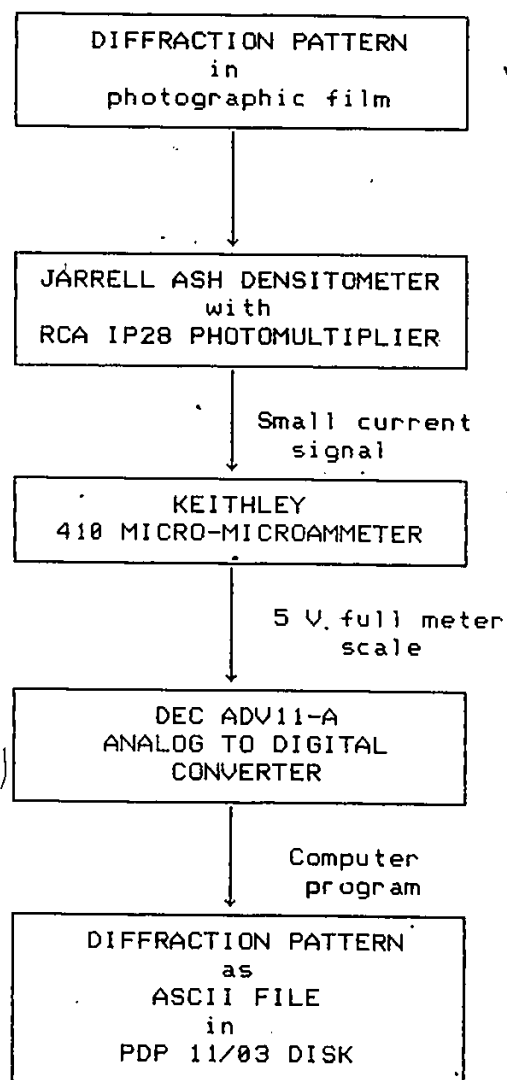


Table II-6 Diffraction pattern recording process

CHAPTER III

Theoretical Considerations

I) Introduction

The derivation of distribution functions from interference patterns of X-rays or electrons for materials containing a single species was first achieved by Zernike and Prins ⁽¹⁰⁾ in 1927. The first application of this technique was carried out in 1930 by Debye and Menke ⁽¹¹⁾ in studying the structure of liquid mercury. Since then a good number of authors ⁽¹²⁻¹⁸⁾ have treated the subject, expanding the theory to cover materials with more than one species.

The aim of this section is to present this theory in a general fashion while trying to give sufficient background to obtain a thorough understanding of the concepts involved in electron diffraction experiments. Let us consider now some of the factors that ought to be taken into consideration when studying the scattering of an electron beam.

The interference pattern obtained by electron diffraction is determined by the manner in which the atoms are distributed in the scattering lattice of the observed sample. Of the various interactions that arise with the passage of an electron beam through the sample, coulombic attraction and repulsion are by far the most significant and thus are the only ones that need be considered. The range and duration of these interactions is short even with respect to atomic magnitudes and by using accelerating potentials in excess of 30 KV the range can be reduced to a level that permits the use of useful approximations. The electron distribution of the individual scattering atoms in the

chapter III: Theoretical Considerations

lattice is assumed to be spherical. The initial beam is described as a parallel electron wave in a spherical atomic force field. With these approximations the Hamiltonian for the system is determined. The corresponding Schrodinger equation describes the way in which the electron wave changes as it passes through the field. On the emerging side of the field the potential energy decreases to zero and the electron wave function will assume an asymptotic form. The scattered beam, as observed at some point remote from the scattering center, is the resultant of all waves emanating from the different atomic centers. Thus the wave function of the beam is obtained by adding the wave functions due to the scattering of the individual atoms. Each of these component waves has traveled a different distance to reach the point of observation and consequently interference effects are observed. On the scale of the observer the scattered beam of electrons can be treated as if it came from a single point, i.e. the wave function has spherical form and its intensity is inversely proportional to the distance from the scattering center.

During the collision process there exists the possibility that either of two different types of events may occur. In one the incoming electron deflects off the target without energy exchange, and in the other there is an energy exchange. These two processes are referred as elastic and inelastic scattering respectively. The elastically scattered electrons retain their original wavelength while inelastically scattered electrons after losing some of their energy obtain a longer wavelength. The difference of wavelengths can be large enough to cause interference.

chapter III: Theoretical Considerations

ference effects between the elastic and inelastic parts of the scattered beam, thus to reduce unwanted interference effects inelastic scattering is always minimized.

II) Atomic Elastic Scattering

i) Classical Treatment

Let us consider first the classical treatment of scattering by a coulombic force field. It should be noted that while many aspects of the classical treatment are inappropriate for atomic scale phenomena, it does nevertheless give estimates of the magnitude of some of the parameters of the problem.

The standard classical treatment which deals with the case of a moving body scattered by an inverse square force field exerted upon it by a stationary object of infinite mass is solved in Goldstein's book (19).

If the moving body has sufficient kinetic energy to avoid capture its path will be hyperbolic. If the force is coulombic and assuming that the moving object is an electron and that the stationary object has a charge of qe then we have the relation:

$$p \tan \theta = \frac{qe^2}{m v_0^2} \quad (1)$$

where m is the mass of the electron, v_0 its initial velocity and p is the impact parameter. The angle of deflection, θ increases with the charge of the scattering atom and decreases with increasing kinetic energy. As a measure of the effective range of the coulombic interaction we can determine the impact parameter corresponding to the smallest measurable deflection under typical experimental conditions. We assume that it is impractical to

chapter III: Theoretical Considerations

measure the intensity of scattered electron beams with scattering angle of less than 1° . If we take that as our minimum measurable deflection assuming that the incident electrons have a kinetic energy of 100KV and that the charge of the scattering atoms is 1, then the maximum impact parameter for which the deflections are significant is less than 0.01 angstroms. Thus the probability that an electron, in its passage through an atomic field, will suffer a measurable deflection is small. Even if the orientation of the crystal lattice with respect to the path of the electron is such that the electron may pass through the force field of more than one atom, it still is unlikely that more than one measurable deflection will take place. This line of thought constitutes at least a qualitative justification for the use of approximations to describe the scattering centres.

ii) The Schroedinger Equation

The target atom is treated as stationary thus the only kinetic energy operator in the Hamiltonian for the system is that of the beam electron. The potential interaction term is that for the beam electron and an atom with a time averaged electron distribution. Since we assumed that the electron distribution had spherical symmetry, the potential energy will be a function of a single variable r , the distance from the beam electron to the atomic nucleus.

The general form of the Schroedinger equation in polar coordinates is

Chapter III: Theoretical Considerations

$$-\frac{h^2}{8\pi^2m} \nabla^2 [R(r)Y(\phi)] + V(r)R(r)Y(\phi) = R(r)Y(\phi)E \quad (2)$$

where

$$\nabla_{r,\phi}^2 = \frac{1}{r^2} \frac{\partial}{\partial r} \left[\frac{r^2 \partial}{\partial r} \right] + \frac{1}{r^2 \sin \phi} \frac{\partial}{\partial \phi} \left[\frac{\sin \phi \partial}{\partial \phi} \right] \quad (3)$$

and $\phi=2\theta$ is the angle of deflection.

The separation of variables is accomplished in the following manner:

$$\begin{aligned} & -\frac{h^2}{8\pi^2m} \left\{ \frac{1}{r^2} \frac{\partial}{\partial r} \left[\frac{r^2 \partial [R(r)Y(\phi)]}{\partial r} \right] \right. \\ & \left. + \frac{1}{r^2 \sin \phi} \frac{\partial}{\partial \phi} \left[\frac{\sin \phi \partial [R(r)Y(\phi)]}{\partial \phi} \right] \right\} + [E - V(r)]R(r)Y(\phi) = 0 \end{aligned} \quad (4)$$

Rearrange to give

$$\begin{aligned} & \frac{Y(\phi)}{r^2} \frac{d}{dr} \left[\frac{r^2 dR(r)}{dr} \right] + \frac{R(r)}{r^2 \sin \phi} \frac{d}{d\phi} \left[\frac{\sin \phi dY(\phi)}{d\phi} \right] \\ & + [k^2 - U(r)]R(r)Y(\phi) = 0 \end{aligned} \quad (5)$$

where

$$k^2 = \frac{8\pi^2mE}{h^2} \quad U(r) = \frac{8\pi^2mV(r)}{h^2} \quad (5a)$$

Multiplying equation (5) by r^2 and dividing by the wave function $R(r)Y(\phi)$ yields:

$$\begin{aligned} & \frac{1}{R(r)} \frac{d}{dr} \left[\frac{r^2 dR(r)}{dr} \right] + [k^2 - U(r)]r^2 = \\ & \frac{1}{-Y(\phi) \sin \phi} \frac{d}{d\phi} \left[\frac{\sin \phi dY(\phi)}{d\phi} \right] \end{aligned} \quad (6)$$

Since the variables are independent, equation (6) can only be satisfied if both sides are equal to a constant. Let this constant be c , then the differential equation for $Y(\phi)$ is

Chapter III: Theoretical Considerations

$$\frac{1}{-Y(\phi)\sin\phi} \frac{d}{d\phi} \left[\frac{\sin\phi dY(\phi)}{d\phi} \right] = -cY(\phi) \quad (7)$$

by making the transformation $X=\cos\phi$ we get

$$\frac{d}{dX} \left[(1-X^2) \frac{dY}{dX} \right] + cY = 0 \quad (8)$$

This is the general form of the Legendre Differential Equation. Solutions to this equation exists if $c=l(l+1)$, where l is a positive integer. The solutions are given by

$$Y(\phi) = P_l(\cos\phi) \quad (9)$$

which are the Legendre polynomials. The functional form of the Legendre polynomials is well known (20).

So far we have found that we are dealing with a system that has quantized eigenstates. The quantum number l , which characterizes these states, is associated with an angular momentum value of $L=[l(l+1)]^{1/2} \hbar$. These are the states available to the individual electrons. The incoming beam will contain electrons distributed among the available states, thus the wave function of the beam will be of the form

$$\Psi(r, \phi) = \sum_{l=0}^{\infty} A_l R_l(r) P_l(\cos\phi) \quad (10)$$

where the coefficients A_l will be determined by suitable boundary conditions.

From equation (6) the radial wave equation can be determined as

$$\frac{1}{R_l(r)} \frac{d}{dr} \left[\frac{r^2 dR_l(r)}{dr} \right] + [k^2 - U(r)]r^2 = l(l+1) \quad (11)$$

which rearranges to

Chapter III: Theoretical Considerations

$$\frac{1}{r^2} \frac{d}{dr} \left[\frac{r^2 dR_1(r)}{dr} \right] + \left[k^2 - U(r) - \frac{l(l+1)}{r^2} \right] R_1(r) = 0 \quad (12)$$

iii) Asymptotic Solution

At large r , $r \rightarrow \infty$, both $U(r)$ and r^{-2} approach zero. Thus the solutions of equation (12) will approach the solutions of

$$\frac{1}{r^2} \frac{d}{dr} \left[\frac{r^2 dR_1(r)}{dr} \right] = -k^2 R_1(r) \quad (13)$$

The general solution of equation (13) is of the form

$$R_1(r) = B_1 r^{-1} \sin(kr) + C_1 r^{-1} \cos(kr) \quad (14)$$

where the coefficients B_1 and C_1 may be real or imaginary.

At small r the functions $R_1(r)$ must also approach the solutions of the equation obtained by setting term $U(r)$ equal to zero in equation (12)

$$\frac{1}{r^2} \frac{d}{dr} \left[\frac{r^2 dR_1(r)}{dr} \right] + \left[k^2 - \frac{l(l+1)}{r^2} \right] R_1(r) = 0 \quad (15)$$

This is a form of the Bessel's equation and its solutions are well known (21). These are of the form

$$R_1(r) = \left[\frac{\pi}{2kr} \right]^{\frac{1}{2}} J_{l+\frac{1}{2}}(kr) = J_l(kr) \quad (16)$$

We are interested in the asymptotic form of the solutions given in equation (16) which are finite for all values of r . This will give us a description of the incident beam since it has suffered no potential interaction. The asymptotic form of the solutions is

Chapter III: Theoretical Considerations

$$R_1(r) = \frac{1}{kr} \sin(kr - \frac{1\pi}{2}) \quad (16a)$$

By inserting equation (16a) into equation (10) and remembering that the incident beam is represented by a plane wave function we obtain

$$\sum_{l=0}^{\infty} A_l R_l(r) P_l(\cos\phi) = e^{ikz} = e^{ikr \cos\phi} \quad (17)$$

To obtain the coefficients A_l we multiply both sides of equation (17) by $P_l(\cos\phi) \sin\phi$ and integrate from 0 to π

$$\int_0^{\pi} P_l(\cos\phi) \sin\phi e^{ikr \cos\phi} d\phi = \int_0^{\pi} A_l R_l(r) P_l^2(\cos\phi) \sin\phi d\phi \quad (18)$$

Letting $t = \cos\phi$ we obtain

$$\begin{aligned} \int_{-1}^1 P_l(t) e^{ikrt} dt &= A_l R_l(r) \int_{-1}^1 P_l^2(t) dt \\ &= \frac{2}{2l+1} A_l R_l(r) \end{aligned} \quad (19)$$

Integrating the left hand side by parts yields

$$\int_{-1}^1 P_l(t) e^{ikrt} dt = \frac{1}{ikr} [e^{ikrt} P_l(t)]_{-1}^{+1} - \frac{1}{ikr} \int_{-1}^1 e^{ikrt} P_l'(t) dt \quad (20)$$

The second term is of the order of r^{-2} and in our asymptotic assumption can be neglected thus

$$\frac{2}{2l+1} A_l R_l(r) = \frac{1}{ikr} [e^{ikrt} P_l(t)]_{-1}^{+1} \quad (21)$$

Since $P_l(1)=1$ and $P_l(-1)=(-1)^l$ the right hand side of equation (21) is

Chapter III: Theoretical Considerations

$$\text{RHS} = \frac{1}{ikr} [e^{ikr} P_1(\cos\theta)]_{-1}^{+1} = \frac{1}{ikr} e^{ikr} - (-1)^1 e^{-ikr} \quad (22)$$

Recall that $(-1)^1 = e^{i\pi}$, thus

$$\begin{aligned} \text{RHS} &= \frac{1}{ikr} [e^{ikr} - e^{i\pi} e^{-ikr}] \\ &= \frac{1}{2kr} \frac{e^{i(kr - \frac{\pi}{2})} - e^{-i(kr - \frac{\pi}{2})}}{2i} \end{aligned} \quad (23)$$

but $e^{i\frac{\pi}{2}} = i$ thus

$$\text{RHS} = \frac{2i}{kr} \sin(kr - \frac{\pi}{2}) \quad (24)$$

Hence equation (21) becomes

$$\frac{2}{2l+1} A_l R_l(r) = \frac{2}{kr} i^l \sin(kr - \frac{\pi}{2}) \quad (25)$$

substituting (16a) in (25) we get

$$\frac{2}{2l+1} A_l \frac{2}{kr} \sin(kr - \frac{\pi}{2}) = \frac{2}{kr} i^l \sin(kr - \frac{\pi}{2})$$

Therefore

$$A_l = (2l+1) i^l \quad (26)$$

and consequently the wave function for the incident beam is

$$e^{ikz} = \sum_{l=0}^{\infty} (2l+1) i^l \frac{1}{kr} \sin(kr - \frac{\pi}{2}) P_l(\cos\theta) \quad (27)$$

iv) The Scattered Beam

As previously stated the wave function of the scattered beam can be considered to have spherical symmetry in which the scattered amplitude $f(\theta)$ will be determined by the nature of the scattering center. A substantial part of the beam that passes

Chapter III: Theoretical Considerations

through the potential field will be undeflected, thus there will be a significant plane wave component. From these consideration we can anticipate that the wave function of the scattered beam will be of the form:

$$\psi(r, \phi) = \frac{1}{r} f(\phi) e^{ikr} + e^{ikz} \quad (28)$$

We approach the problem of finding the asymptotic form of the scattered wave function in the same manner as we did for the incident beam. The angular dependence for both incident and scattered beams are the same, thus the angular functions will again be the Legendre polynomials. The radial functions must be solutions of both equations (13) and (15), furthermore the radial functions must approach the form given in equation (16a) as $U(r)$ becomes vanishingly small. However unlike the incident beam, the scattered beam has a past history arising from its passage through the atomic field, thus it can be determined (22) that the radial part of the scattered beam wave function has the form

$$R_l(r) = \frac{1}{kr} \sin(kr - \frac{\pi l}{2} + \eta_l) \quad (29)$$

where η_l is called the partial wave phase shift and depends on k and $U(r)$. We can now write the wave function as

$$\psi(r, \phi) = \sum_{l=0}^{\infty} A_l P_l(\cos \phi) \frac{1}{kr} \sin(kr - \frac{\pi l}{2} + \eta_l) \quad (30)$$

Substituting equation (28) in (30)

$$\begin{aligned} \sum_{l=0}^{\infty} A_l P_l(\cos \phi) \frac{1}{kr} \sin(kr - \frac{\pi l}{2} + \eta_l) \\ = \frac{1}{r} f(\phi) e^{ikr} + e^{ikr \cos \phi} \end{aligned} \quad (31)$$

Chapter III: Theoretical Considerations

substituting the plane wave expansion of equation (27) yields

$$\begin{aligned}
 & - \sum_{l=0}^{\infty} A_l P_l(\cos\phi) \frac{1}{kr} \sin(kr - \frac{\pi l}{2} + \eta_l) \\
 & = \frac{1}{r} f(\phi) e^{ikr} + \sum_{l=0}^{\infty} (2l+1) i^l \sin(kr - \frac{\pi l}{2}) P_l(\cos\phi)
 \end{aligned} \tag{32}$$

rearranging

$$\begin{aligned}
 & \sum_{l=0}^{\infty} \frac{1}{kr} P_l(\cos\phi) \left[A_l \sin(kr - \frac{\pi l}{2} + \eta_l) - (2l+1) i^l \sin(kr - \frac{\pi l}{2}) \right] \\
 & = \frac{1}{r} f(\phi) e^{ikr}
 \end{aligned} \tag{33}$$

Equation (33) represents the spherical part of the scattered wave function. We have to choose the A_l coefficients so that the LHS of the equation will only have terms containing $\exp(ikr)$. Consider the term in brackets in equation (33)

$$\begin{aligned}
 T &= A_l \sin(kr - \frac{\pi l}{2} + \eta_l) - (2l+1) i^l \sin(kr - \frac{\pi l}{2}) \\
 &= A_l \frac{e^{i(kr - \frac{l\pi}{2})} e^{i\eta_l} - e^{-i(kr - \frac{l\pi}{2})} e^{i\eta_l}}{2i} \\
 &\quad - (2l+1) i^l \left[\frac{e^{i(kr - \frac{l\pi}{2})} - e^{-i(kr - \frac{l\pi}{2})}}{2i} \right]
 \end{aligned} \tag{34}$$

collecting terms

$$\begin{aligned}
 T &= \frac{1}{2i} \left[e^{i(kr - \frac{l\pi}{2})} \left(A_l e^{i\eta_l} - (2l+1) i^l \right) \right. \\
 &\quad \left. - e^{-i(kr - \frac{l\pi}{2})} \left(A_l e^{-i\eta_l} - (2l+1) i^l \right) \right]
 \end{aligned} \tag{35}$$

consequently by the previously stated conditions

Chapter III: Theoretical Considerations

$$A_1 e^{-i\eta_1} - (2l+1)i^l = 0$$

hence

$$A_1 = (2l+1)i^l e^{i\eta_1} \quad (36)$$

Substituting equations (35) and (36) in (33)

$$\frac{1}{r} f(\phi) e^{ikr} = \quad (37)$$

$$\sum_{l=0}^{\infty} \frac{1}{kr} P_l(\cos\phi) \frac{1}{2i} e^{i(kr - \frac{l\pi}{2})} (2l+1)i^l (e^{2i\eta_1} - 1)$$

thus

$$f(\phi) = \sum_{l=0}^{\infty} \frac{1}{2ik} P_l(\cos\phi) e^{-\frac{l\pi}{2}} i^l (2l+1) (e^{2i\eta_1} - 1) \quad (38)$$

$$\text{and since } i^l = e^{\frac{l\pi}{2}}$$

$$f(\phi) = \frac{1}{2ik} \sum_{l=0}^{\infty} (2l+1) (e^{2i\eta_1} - 1) P_l(\cos\phi) \quad (39)$$

this expression gives us the amplitude of the scattered electron wave.

v) The Born Approximation

The determination of the scattering amplitudes $f(\phi)$ requires the evaluation of all the partial wave shifts η_l . Consider then the term in equation (39) which contains the wave shifts

$$e^{i\eta_1} - 1 = 2i\eta_1 + 2i^2\eta_1^2 + \frac{1}{3} 4i^3\eta_1^3 + \dots \quad (40)$$

Provided that the wave shifts are small this series will

Chapter III: Theoretical Considerations

converge in a small number of terms. The Born approximation consists of taking into account the first term of the series only. Since we can expect the magnitude of the phase shifts to increase with atomic interaction it stands to reason that this approximation works best for fast moving electron beams, specifically those with an accelerating potential of greater than about 30KV. Substituting the approximation into equation (39) we get

$$f(\phi) = \frac{1}{k} \sum_{l=0}^{\infty} (2l+1) \eta_l P_l(\cos\phi) \quad (41)$$

It should be noted that scattering amplitudes are no longer complex, however as the equation stands it is still necessary to evaluate each of the partial wave shifts η_l to calculate $f(\phi)$. As previously stated the Born approximation assumes that the partial waves shifts are small which implies that the potential interaction brings only small modifications to the electron beam. This suggests the use of perturbation techniques to solve the differential equation (12) that provide us with the electron beam wave functions. Thus, assume the radial wave function to be the sum of a dominant plane wave term and a small perturbation. To simplify notation we make the following transformation

$$R_l(r) = \frac{1}{r} G_l(r) \quad (42)$$

Equation (12) now becomes

$$G_l''(r) + [k^2 - U(r) - \frac{l(l+1)}{r^2}] G_l = 0 \quad (43)$$

where the dashes denote differentiation with respect to r . We assume that the solutions are of the form

$$G_l(r) = g_l(r) + w(r) \quad (44)$$

Chapter III: Theoretical Considerations

where $g_1(r)$ are the solution of equation

$$g_1''(r) + [k^2 - \frac{1(1+1)}{r^2}]g_1 = 0$$

and they are of the form

$$g_1(r) = \left[\frac{\pi kr}{2} \right]^{\frac{1}{2}} J_{1+\frac{1}{2}}(kr) \quad (45)$$

$w(r)$ is the small perturbation term.

Substituting in equation (43) we obtain

$$\begin{aligned} g_1''(r) + [k^2 - \frac{1(1+1)}{r^2}]g_1 \\ + w'' + [k^2 - \frac{1(1+1)}{r^2}]w = U(r)g_1 + U(r)w \end{aligned} \quad (46)$$

The term in the first line of the equation is zero and neglecting the small term $U(r)w$ we get

$$w'' + [k^2 - \frac{1(1+1)}{r^2}]w = U(r)g_1 \quad (47)$$

Let $w(r) = g_1(r)h(r)$. Thus

$$h''g_1 + 2g_1'h' + h \left[g_1'' + [k^2 - \frac{1(1+1)}{r^2}]g_1 \right] h = U(r)g_1 \quad (48)$$

which reduces to

$$h''g_1 + 2g_1'h' = U(r)g_1 \quad (49)$$

multiplying (49) by $g_1(r)$ and integrating we get

$$\begin{aligned} [h'g_1^2] &= U(r)g_1^2(r) \\ h'g_1^2 &= \int_0^r U(r)g_1^2(r) dr \end{aligned} \quad (50)$$

For large r we have already seen that $g_1 \propto \sin(kr - \frac{\pi}{2})$,

Chapter III: Theoretical Considerations

as $r \rightarrow \infty$

$$\frac{dh}{dr} \propto \frac{1}{\sin^2(kr - \frac{\pi l}{2})} \int_0^\infty U(r) g_1^2(r) dr \quad (51)$$

Let the integral be denoted by A_1 . This integral converges and its value is small (22). Thus integrating equation (51) yields

$$h \propto -\frac{A_1}{k} \left[\cot(kr - \frac{\pi l}{2}) + C \right] \quad (52)$$

where C is a constant. Hence $G_1 = g_1 + g_1 h$ becomes

$$G_1 \propto \sin(kr - \frac{\pi l}{2}) - \frac{A_1}{k} \left[\cos(kr - \frac{\pi l}{2}) + C \sin(kr - \frac{\pi l}{2}) \right] \quad (53)$$

Since $\frac{A_1}{k}$ is small

$$\cos \frac{A_1}{k} \approx 1 \quad \text{and} \quad \sin \frac{A_1}{k} \approx \frac{A_1}{k}$$

neglecting the smaller order terms we have that

$$G_1 \propto \sin(kr - \frac{\pi l}{2} + \eta_1) \quad (54)$$

$$\text{where } \eta_1 = -\frac{A_1}{k} \quad (55)$$

Expanding equations (55) we get

$$\eta_1 = -\frac{1}{k} \int_0^\infty U(r) g_1^2(r) dr$$

Substituting equations (5a) and (45)

$$\eta_1 = \frac{-1}{k} \int_0^\infty \frac{8\pi^2 m}{h^2} V(r) \frac{\pi k r}{2} J_{1+\frac{1}{2}}^2(kr) dr$$

$$= \frac{4\pi^3}{h^2} m \int_0^\infty V(r) J_{1+\frac{1}{2}}^2(kr) r dr$$

$$= \frac{4\pi^3}{h^2} m \int_0^\infty V(r) \frac{2kr}{\pi} J_1^2 r dr$$

therefore

$$\eta_1 = \frac{8\pi^2 km}{h^2} \int_0^\infty V(r) J_1^2 r^2 dr \quad (56)$$

Consider now the well known expansion (23)

$$\frac{\sin(Kr)}{Kr} = \sum_{l=0}^{\infty} (2l+1) P_l(\cos\phi) J_l^2 \quad (57)$$

$$\text{where } K = \frac{4\pi \sin\theta}{\lambda}$$

Substituting equation (57) in (56)

$$\eta_1 = \frac{8\pi^2 km}{h^2} \left[\sum_{l=0}^{\infty} (2l+1) P_l(\cos\phi) \right]^{-1} \int_0^\infty V(r) \frac{\sin Kr}{Kr} r^2 dr \quad (58)$$

and finally substituting into equation (41) we get

$$f(\phi) = \frac{8\pi^2 m}{h^2} \int_0^\infty V(r) \frac{\sin Kr}{Kr} r^2 dr \quad (59)$$

Now we have the scattering amplitudes in terms of only the potential for the interaction of the electron beam and the atom. The calculations of the potential and consequently of the $f(\phi)$, which are referred to as atomic scattering factors, have been calculated by a number of authors and their values have been tabulated. In this study we have used the scattering factors given by Doyle and Turner (24).

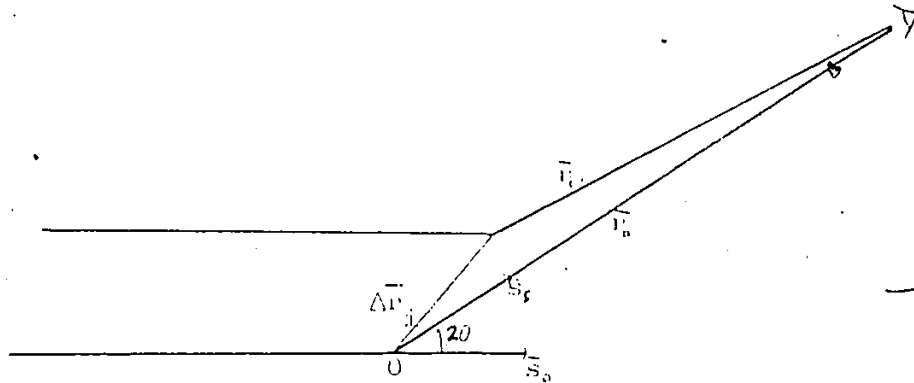
Chapter III: Theoretical Considerations

III) Scattering by an Ensemble of Atoms

The beam scattered by one of the atoms in an ensemble of N atoms is represented by the wave function

$$\psi_i(r_i, \theta) = e^{ikz_i} + \frac{1}{r} f_i(\theta) e^{ikr_i} \quad (60)$$

where $\theta = \angle \theta$ is the angle of deflection and both r_i and z_i have their origin at the nucleus of the i th atom. To determine the scattering of the lattice we shall express all the wave functions in terms of variables with a common origin. Consider the following diagram



where O represents some arbitrary but common origin.

Let \bar{s}_0 be the unit vector in the incoming beam direction

\bar{s}_s be the unit vector in the direction of the scattering

$$\bar{S} = \bar{s}_0 - \bar{s}_s, \text{ thus } |\bar{S}| = S = 2\sin\theta$$

and we denote $\Delta z_i = z_0 - z_i$

We change origins by multiplying equation (60) with $\exp(ik\Delta z_i)$, thus

$$\psi_i(r_i, \theta) = e^{ikz_0} + \frac{1}{r} f_i(\theta) e^{ik\Delta z_i} e^{ik(|\bar{r}_0 - \Delta \bar{r}_i|)}$$

Chapter III: Theoretical Considerations

$$\begin{aligned}
 &= e^{ikz_0} + \frac{1}{r} f_i(\theta) e^{ik\bar{s}_0 \cdot \bar{r}_i} e^{ik(\bar{r}_0 - \bar{r}_i \cdot \bar{s})} \\
 &= e^{ikz_0} + \frac{1}{r} f_i(\theta) e^{ik\bar{r}_i \cdot (\bar{s}_0 - \bar{s}_i)} e^{ikr_0} \quad (61)
 \end{aligned}$$

The wave function representing the scattering from the whole ensemble of atoms is the sum of the wave functions of the contributing atoms

$$\psi(r, \theta) = \sum_{i=0}^N \psi_i(r_i, \theta) \quad (62)$$

Consequently the intensity of the scattered beam is

$$I(r, \theta) = \sum_{i,j}^N f_i^*(\theta) f_j(\theta) e^{ik\bar{s} \cdot \bar{r}_{ij}} \quad (63)$$

Where the vector $\bar{r}_{ij} = \bar{r}_j - \bar{r}_i$. Its magnitude is the distance separating the i th and the j th atoms. In this expression there will be N terms for which $i=j$ and $r_i=r_j$ for each of these terms the exponential would be unity, this allows us to rewrite the expression as

$$I = \sum_{i=1}^N |f_i|^2 + \sum_{\substack{i,j \\ i \neq j}}^N f_i f_j e^{ik\bar{s} \cdot \bar{r}_{ij}} \quad (64)$$

But as we have seen in the previous section under the Born approximation the atomic scattering factors, $f(\theta)$, are real, thus

$$I = \sum_{i=1}^N f_i^2 + \sum_{\substack{i,j \\ i \neq j}}^N f_i f_j e^{ik\bar{s} \cdot \bar{r}_{ij}} \quad (65)$$

This is quite a general result for any ensemble of atoms,

Chapter III: Theoretical Considerations

periodic or not. If the ensemble of atoms were part of a lattice for a crystalline material r_{ij} would take a specific set of values and equation (65) would yield a diffraction function with sharp and well defined peaks. On the other hand if we are dealing with a more amorphous material r_i may be oriented in any direction relative to s with equal probability. In this case the exponential term containing r_{ij} is averaged over all directions

$$\langle e^{ik\vec{s} \cdot \vec{r}_{ij}} \rangle = \frac{1}{4\pi r_{ij}^2} \int_0^\pi e^{ikSr_{ij}\cos\alpha} 2\pi r_{ij}^2 \sin\alpha d\alpha = \frac{\sin(kSr_{ij})}{kSr_{ij}} \quad (66)$$

Letting $s = \frac{2\sin\theta}{\lambda}$ we get

$$I = \sum_{j=1}^N f_j^2 + \sum_{i=1}^N \sum_{\substack{j=1 \\ i \neq j}}^N f_i f_j \frac{\sin 2\pi s r_{ij}}{2\pi s r_{ij}} \quad (67)$$

In most cases the number of species in the sample is small, but the total number of atoms hit by the beam is always very large and this allows us to replace the summation by integration over radial distribution functions $4\pi r^2 \rho_{ij}(r)$, representing the number of j type atoms surrounding an i type atom at distance r . Letting $x_1, x_2, x_3, \dots, x_n$ be the atomic fraction of atoms having scattering factors f_1, f_2, \dots, f_n , where n is the number of species then

$$I(s) = N \sum_{i=1}^n x_i f_i^2 + N \sum_{i=1}^n \sum_{j=1}^n x_i f_i f_j \int_0^\infty 4\pi r^2 \rho_{ij}(r) \frac{\sin 2\pi s r}{2\pi s r} dr \quad (68)$$

We break the integral in the following manner

Chapter III: Theoretical Considerations

$$\begin{aligned}
 I(s) = & N \sum_{i=1}^n x_i f_i^2 \\
 & + N \sum_{i=1}^n \sum_{j=1}^n x_i f_i f_j \int_0^{\infty} 4\pi r^2 [\rho_{ij}(r) - \bar{\rho}_{ij}] \frac{\sin 2\pi sr}{2\pi sr} dr \\
 & + N \sum_{i=1}^n \sum_{j=1}^n x_i f_i f_j \int_0^{\infty} 4\pi r^2 \bar{\rho}_{ij} \frac{\sin 2\pi sr}{2\pi sr} dr
 \end{aligned}$$

where $\bar{\rho}_{ij}$ is the average density. The last term has only a very small contribution for small angles ⁽²⁵⁾, in most cases this contribution is unobservable since it is lost in the undeflected beam. However measurable contribution in the small angle regime may arise if the sample contains regions of excess or deficient density ⁽²⁶⁾, but under normal circumstances the third term can be neglected and hence

$$\begin{aligned}
 I(s) = & N \sum_{i=1}^n x_i f_i^2 \tag{70} \\
 & + N \sum_{i,j} x_i f_i f_j \int_0^{\infty} 4\pi r^2 [\rho_{ij}(r) - \bar{\rho}_{ij}] \frac{\sin 2\pi sr}{2\pi sr} dr
 \end{aligned}$$

Equation (70) gives us the intensity profile of the scattered beam when the sample contains any number of species. In this study we are only interested in samples with one species only thus we can reduce the equation to give

$$\begin{aligned}
 I(s) = & N f^2(s) + N f^2(s) \int_0^{\infty} 4\pi r^2 [\rho(r) - \rho_0] \frac{\sin 2\pi sr}{2\pi sr} dr \\
 = & N f^2(s) \left[1 + \frac{2}{s} \int_0^{\infty} r [\rho(r) - \rho_0] \sin 2\pi s r dr \right] \tag{71}
 \end{aligned}$$

Rearrange to give

Chapter III: Theoretical Considerations

$$s \left[\frac{I(s)}{Nf^2(s)} - 1 \right] = 2 \int_0^{\infty} r[\rho(r) - \rho_0] \sin 2\pi s r dr \quad (72)$$

The reduced interference functions $i(s)$ is defined as

$$i(s) = s \left[\frac{I(s)}{Nf^2(s)} - 1 \right] \quad (73)$$

such that

$$i(s) = 2 \int_0^{\infty} r[\rho(r) - \rho_0] \sin 2\pi s r dr \quad (74)$$

which has the form of a Sine Fourier Transform with the inversion formula of

$$r[\rho(r) - \rho_0] = 2 \int_0^{\infty} i(s) \sin 2\pi s r ds \quad (75)$$

Therefore, the reduced radial distribution function defined as

$$G(r) = 4\pi r[\rho(r) - \rho_0] \quad (76)$$

is given by

$$G(r) = 8\pi \int_0^{\infty} i(s) \sin 2\pi s r ds \quad (77)$$

and finally the radial distribution function is

$$RDF(r) = 4\pi r^2 \rho(r) = 4\pi r^2 \rho_0 + 8\pi r \int_0^{\infty} i(s) \sin 2\pi s r ds \quad (78)$$

CHAPTER IV

Data Analysis

The diffraction data acquired contained random high frequency noise, probably caused by the detection apparatus. In the region of large s the ratio of signal to noise is quite small (1-2), hence it is of primary importance to be able to remove this random noise without degrading the underlying information.

The standard technique used to eliminate random errors is simple averaging of a large number of runs. The main disadvantage of only using averaging is the time involved in the data collection, specially, as in this study, each run takes a few minutes to complete. The use of combined smoothing and averaging considerably reduces the instrument time required. A characteristic of both procedures is that the noise is reduced approximately as the square root of the number of points used. Thus if it is desired to improve the signal to noise ratio by a factor of 10, simple averaging would require a total of 100 runs. On the other hand, a similar improvement can be achieved by making only 16 runs and a 9-point least square smooth

16 runs $\approx 4\times$ improvement

9-point smooth $\approx 3\times$ improvement

The least square smoothing technique used in this study is that described by Savitzky et.al. (27), and the actual programs used are listed in Appendix 2. In addition to random errors the interference curves obtained are subject to a number of systematic errors, each of which must be corrected before calculating the distribution functions. The systematic errors can be

Chapter IV: Data Analysis

divided into the following categories depending on their origin.

There are those arising from:

- 1) Non linear film response
- 2) Termination effects.
- 3) Improper normalization of the interference pattern.
- 4) Effects due to non elastic electron collisions

Each of these will be treated in detail in this chapter

i) Non Linear Film Response

Before starting this discussion a few quantities pertaining to photographic film response ought to be defined⁽²⁸⁾.

- Diffuse Density, this is the density of silver particles per unit volume in the developed photographic emulsion. It is given by the following version of Beer's Law

$$D(s) = \log_{10} \frac{T_{\max}}{T(s)} \quad (79)$$

where T_{\max} corresponds to 100% transmission, i.e. the transmission of a part of film that has not been exposed to either light or the electron beam. $T(s)$ is the transmission function corresponding to the diffraction pattern, in our case this would be the output of our densitometer.

-Exposure, this is defined by the reciprocity law, formulated by Bunsen and Roscoe⁽²⁸⁾ which states that the product of a photochemical reaction is dependent on the total energy involved, thus

$$E = It \quad (80)$$

where E is the exposure

I is the intensity

t is the time of exposure

This is generally true for photographic materials except for exposures of very low or of very high levels of intensity. This loss of intensity is known as the reciprocity effect. The largest deviations from the normal occur at exposures of low intensities. In this work the intensities employed were sufficiently large so that we can expect equation (80) to hold.

The plot of the diffuse density versus the exposure is called the characteristic curve of the film and it varies consi-

derably from one type of film to another, however characteristic curves have features that are common to all (see figure IV-1). These are 1) The Toe, where the density rises very slowly with increasing intensity. 2) The Linear region, where the densities are linearly proportional to the intensities. 3) The Saturation region, where the slope of the curve decreases with increasing intensity, this corresponds to the situation where the incident electrons fail to encounter silver ions that have not been previously excited.

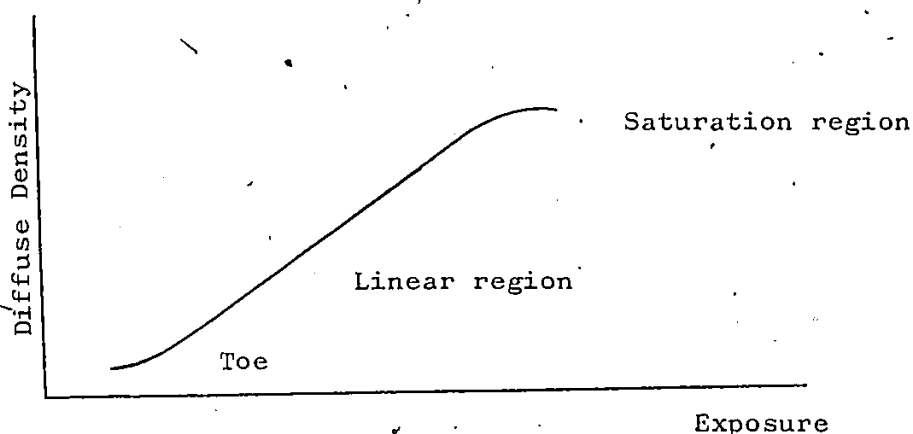


Figure IV-1 Typical characteristic curve for photographic film

The major problem that arises from the usage of photographic film for the recording of diffraction patterns is its inability to respond linearly to all the intensities that may be present in a given pattern. Typically the difference between the lowest and highest peak intensity may vary up to five orders of magnitude and this is larger than the linear range of most films.

Hence it is desirable to find the time of exposure that would yield a picture in which all peaks of the diffraction

Chapter IV: Data Analysis

pattern would be recorded in the linear region or as close to it as possible. To accomplish this the following procedure was adapted. Using a single sample a series of pictures with different exposure times was taken. Special care was taken such that no setting in the electron microscope was changed assuring equal beam intensity for all pictures (see figures IV-2, IV-3). From the corresponding densitometer curves a diffuse density versus exposure curve was constructed for the different distinct peaks in the diffraction pattern (see figures IV-4). In the linear region of these plots the slope is given by

$$m = \frac{\Delta D}{\Delta t} \quad (81)$$

from equation (80) we have $t = E/I$ since I is constant within each curve

$$\Delta t = \frac{\Delta E}{I} \quad (82)$$

hence

$$m = \frac{\Delta D}{\Delta E} I \quad (83)$$

where $\Delta D/\Delta E$ is the slope of the characteristic curve and consequently we see that any change in the slope in the curves in figure IV-4 must be due to a change in the slope in the characteristic curve, i.e. a deviation from the linear region.

A close examination of figure IV-4 reveals that the only exposure time for which the intensity of all peaks fall in the linear region is 0.12 sec, this exposure time was then repeatedly used in all pictures taken.

Figures IV-2, IV-3 Series of diffraction pattern curves of the same sample taken with varying exposure time

Figure IV-4 Plot of diffuse density vs. exposure time for the different well defined peaks present in figures IV-2 and IV-3

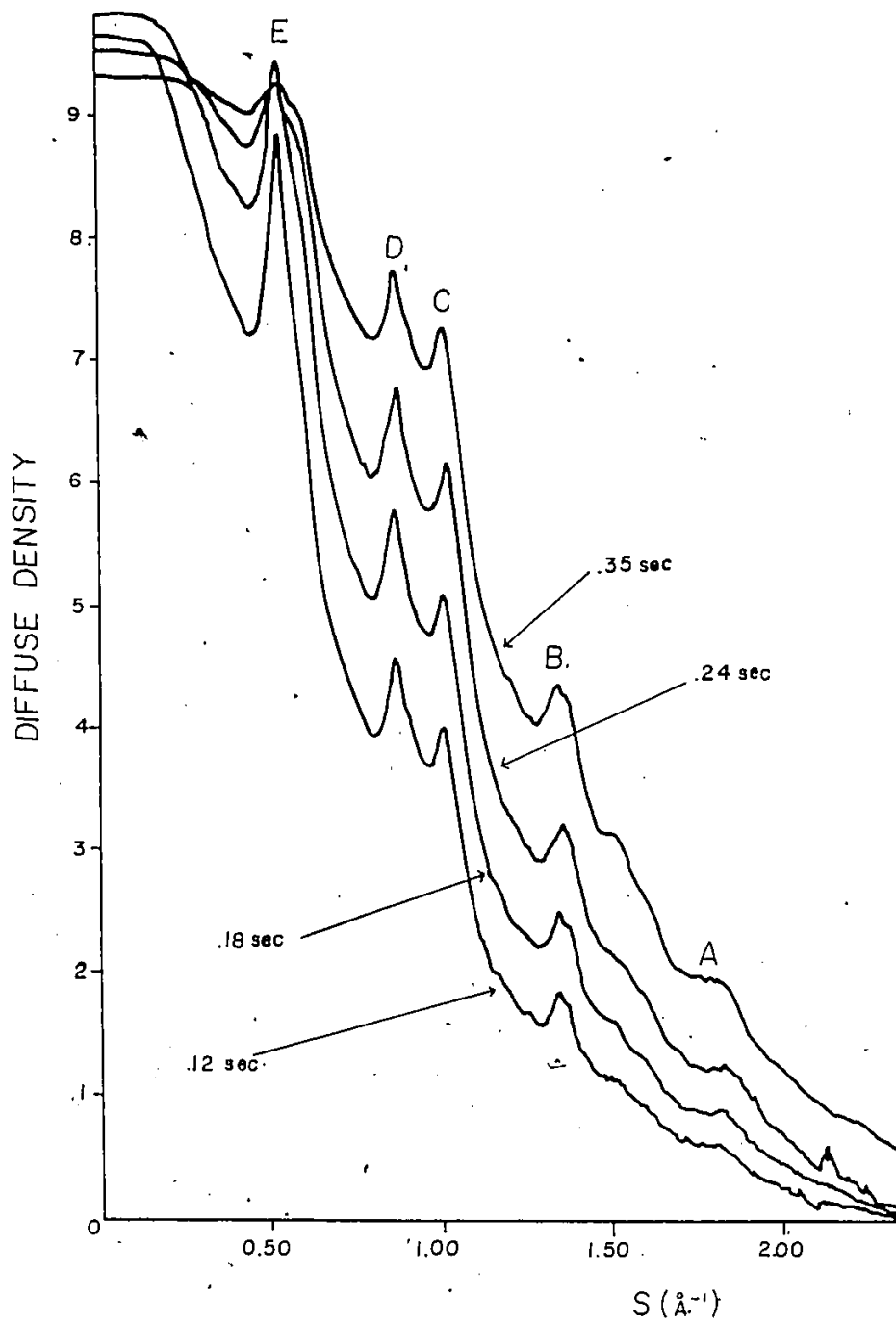


Figure IV-2

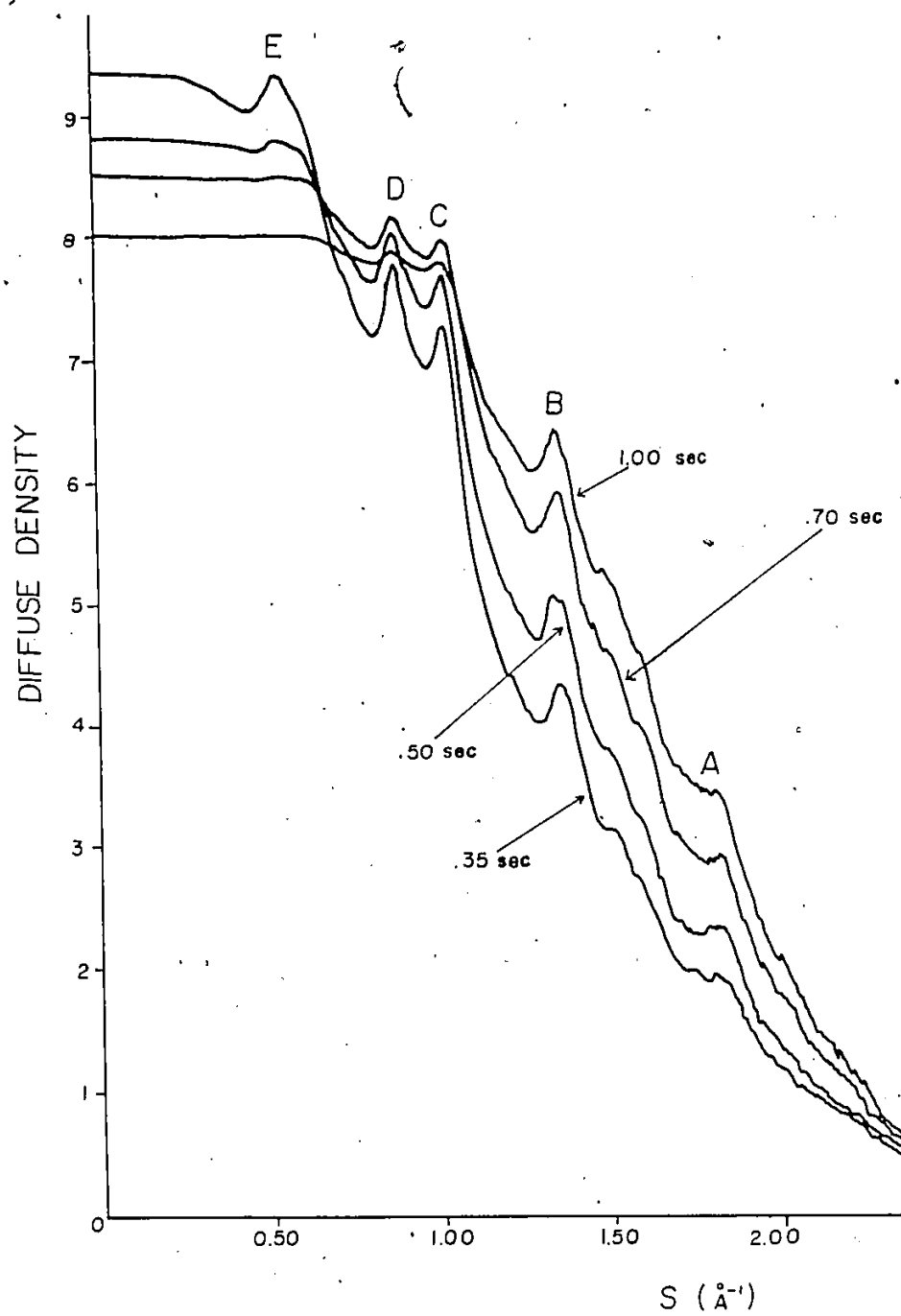


Figure IV-3

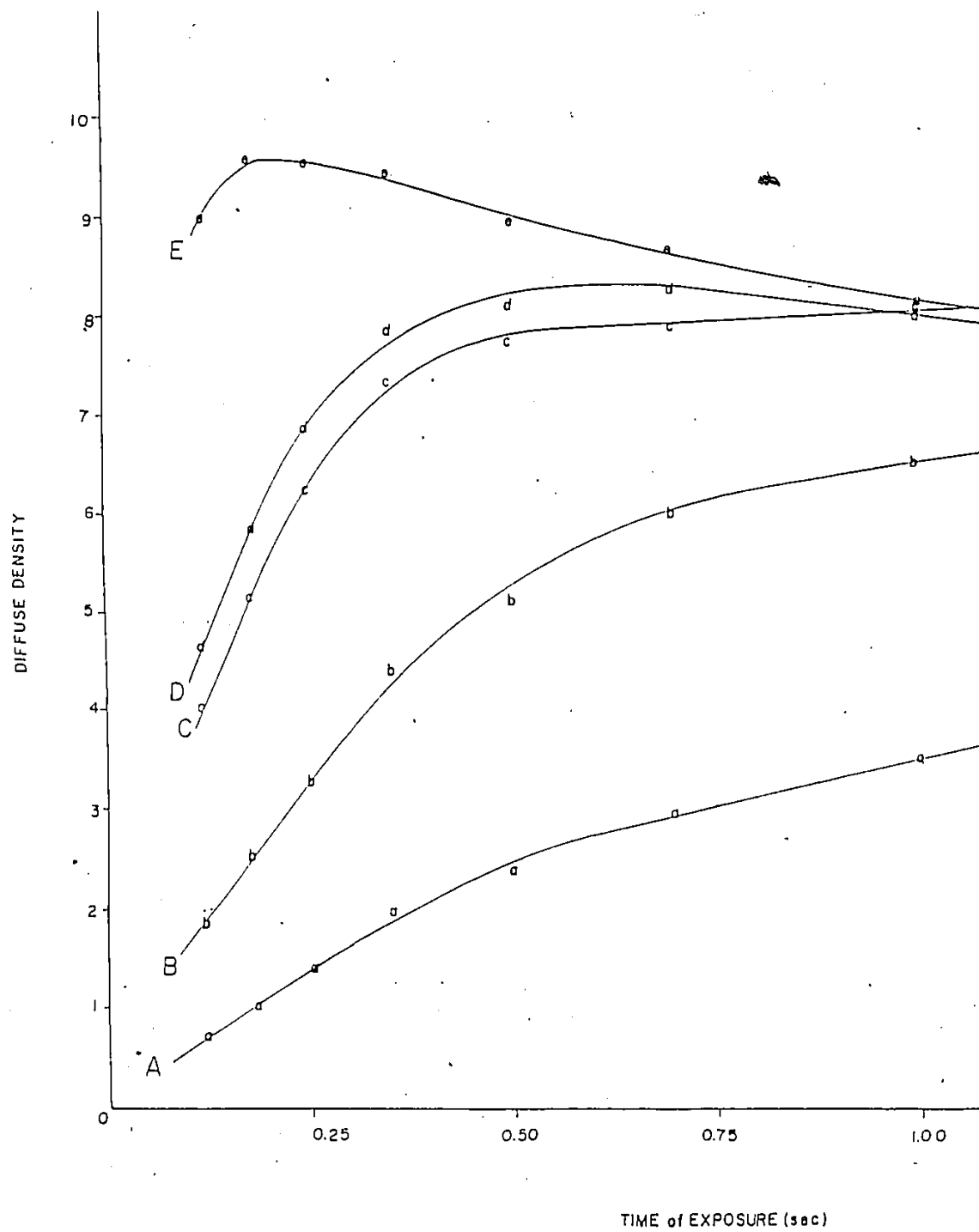


Figure IV-4

ii) Termination Effects

Consider equation (77) which states

$$G(r) = 8\pi \int_0^{\infty} i(s) \sin 2\pi s r ds$$

To accurately determine the reduced radial distribution function, $G(r)$, an integration up to infinity is to be calculated. This leads to the obvious problem: the experimental data is finite and only allows the integration to be carried out up to s_{\max} , the maximum value of the scattering parameter. The question that arises is, what effects does the termination of s have on $G(r)$?

We can think of the truncation of the upper limits in the integral as having multiplied $i(s)$ by a "terminating" function $g(s)$. The terminating function will have the property that it will equal zero for all values of s above s_{\max} . Thus we have in practice

$$G_t(r) = 8\pi \int_0^{\infty} Y(s) \sin 2\pi s r ds \quad (84)$$

where $Y(s) = i(s)g(s)$

Let's adopt the following notation

$$G_t(r) \Leftrightarrow Y(s)$$

where \Leftrightarrow denotes a Fourier Transformation.

We then have the following Fourier transform pairs:

$$G_t(r) \Leftrightarrow Y(s) = i(s)g(s)$$

$$g(s) \Leftrightarrow h(r)$$

$$i(s) \Leftrightarrow G(r)$$

Recall now the form of the convolution integral which is defined as (29)

$$w(t) = \int_{-\infty}^{\infty} x(\tau) y(t-\tau) d\tau = x(t) * y(t) \quad (85)$$

where $*$ denotes convolution.

The convolution theorem (29,30) states that if we have Fourier transform pairs

$$y(t) \Leftrightarrow Y(f) \text{ and } x(t) \Leftrightarrow X(f)$$

then

$$x(t) * y(t) \Leftrightarrow X(f) Y(f)$$

For our particular case

$$Y(s) = i(s) g(s)$$

$$\begin{matrix} \Downarrow & \Downarrow & \Downarrow \\ G_t(r) & = & G(r) * h(r) \end{matrix}$$

thus

$$G_t(r) = \int_0^{\infty} h(r - r') G(r') dr' \quad (86)$$

In the simplest case in which we have just the experimental $i(s)$, the termination function is a square wave pulse defined by

$$\begin{aligned} g(s) &= 1 \quad |s| \leq s_{\max} \\ &= 0 \quad |s| > s_{\max} \end{aligned}$$

its Fourier transform, commonly referred to as the "modifying" function, is given by

$$h(r) = 2s_{\max} \frac{\sin 2\pi s_{\max} r}{2\pi s_{\max} r} = 2s_{\max} \text{sinc}(2\pi s_{\max} r) \quad (87)$$

Figure IV-5 shows the Fourier transform pair $g(s) \Leftrightarrow h(r)$. Thus

$$G_t(r) = 16\pi s_{\max} \int_0^{\infty} \frac{\sin 2\pi s_{\max} (r-r')}{2\pi s_{\max} (r-r')} G(r') dr \quad (88)$$

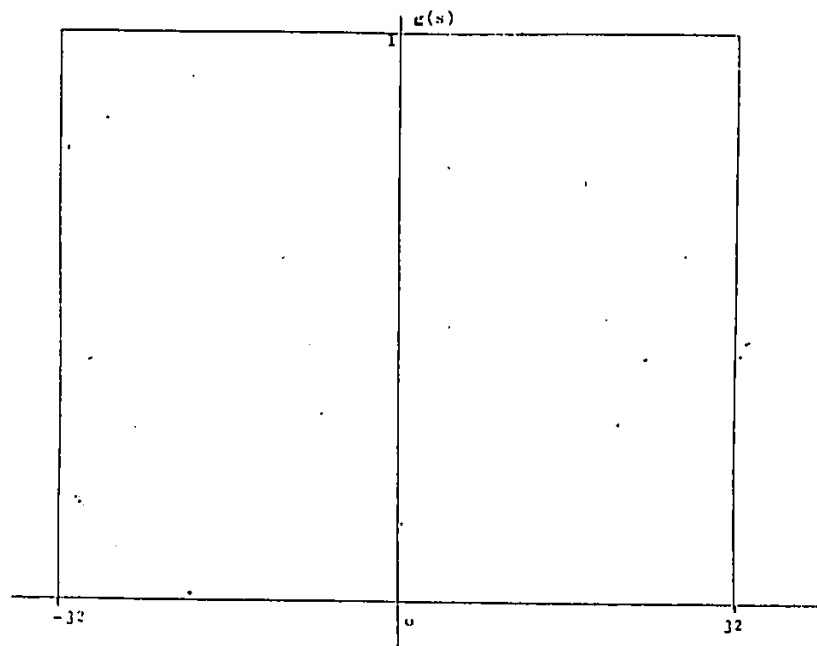
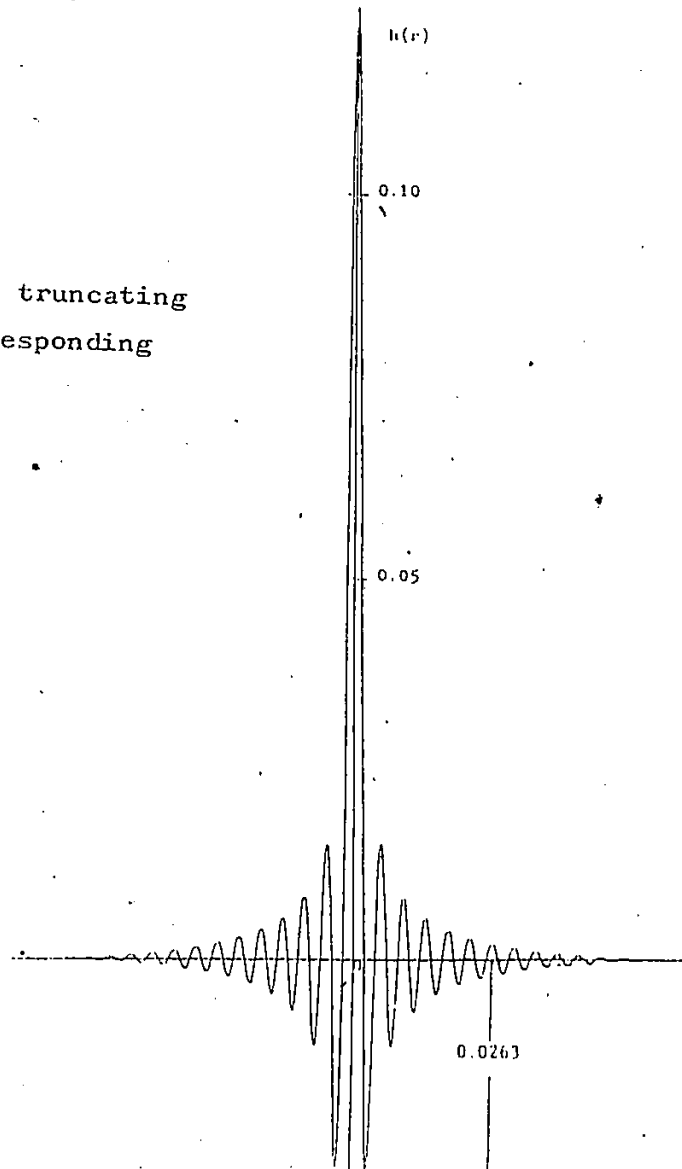


Figure IV-5

Square Wave Pulse truncating
function and corresponding
Fourier transform



In equation (88) $G(r')$ is the ideal reduced radial distribution function which would be obtained if there was no termination, and $G_t(r)$ is the "somewhat" modified function we obtain using the experimental data. The effect of the modifying function is twofold; first it broadens all peaks and second, and most important, it generates spurious peaks, referred to as ripples, which may be mistaken for real information. In order to minimize such ripples the most convenient method is to use a terminating function whose Fourier transform contains oscillations of smaller amplitude than those of the sinc function. Two functions that comply with such criteria are the triangular and hanning function (figures IV-6, IV-7). The triangular function is particularly useful for cases in which negative oscillations are undesirable, as in Fourier spectroscopy. Another point to be considered is the fact that each terminating function broadens the peaks of $G(r)$ by different amounts. Bell⁽³¹⁾ gives the following list comparing the full width at half maximum of the main peak of the modifying function corresponding to some of the most frequently used terminating functions

Terminating function	% increase in FWHM
square wave pulse	0
hanning $[0.5 + 0.5 \cos(\pi s / 2s_{\max})]$	31
triangular $[1 - s / s_{\max}]$	48
square triangular $[1 - (s / s_{\max})^2]^2$	58

The hanning function was the terminating function used in this study for it not only suppresses all ripples but it introduces the least amount of broadening

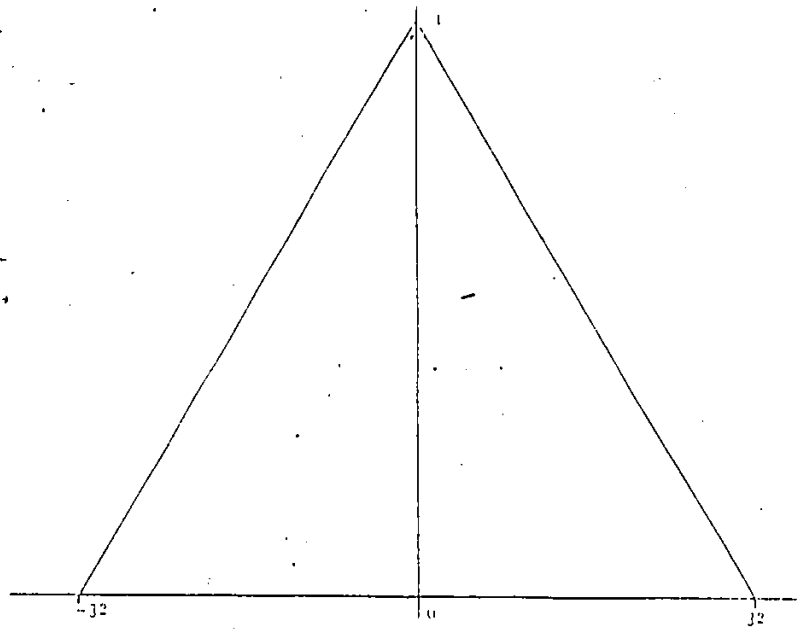
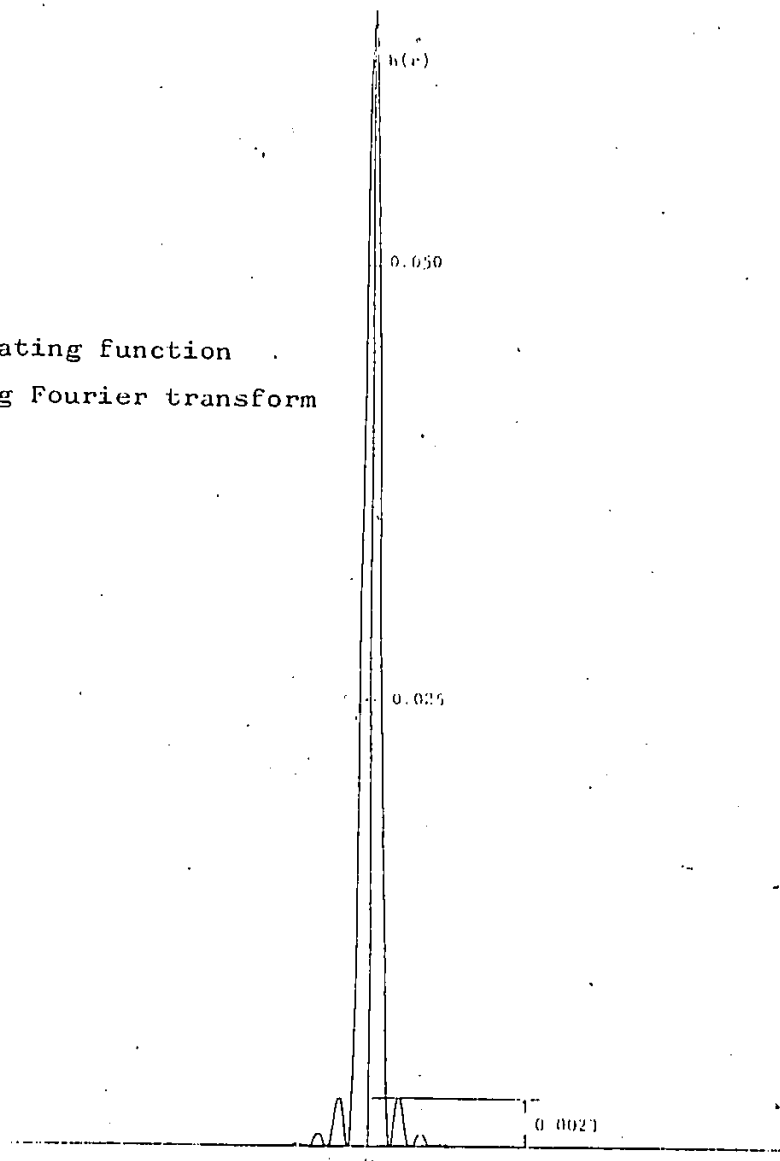


Figure IV-6
 Triangular truncating function
 and corresponding Fourier transform



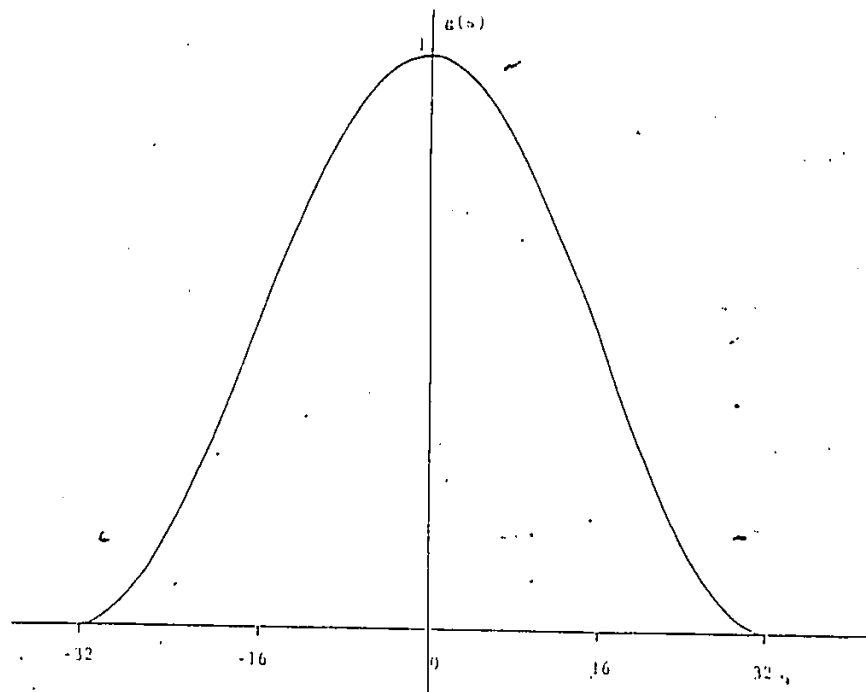
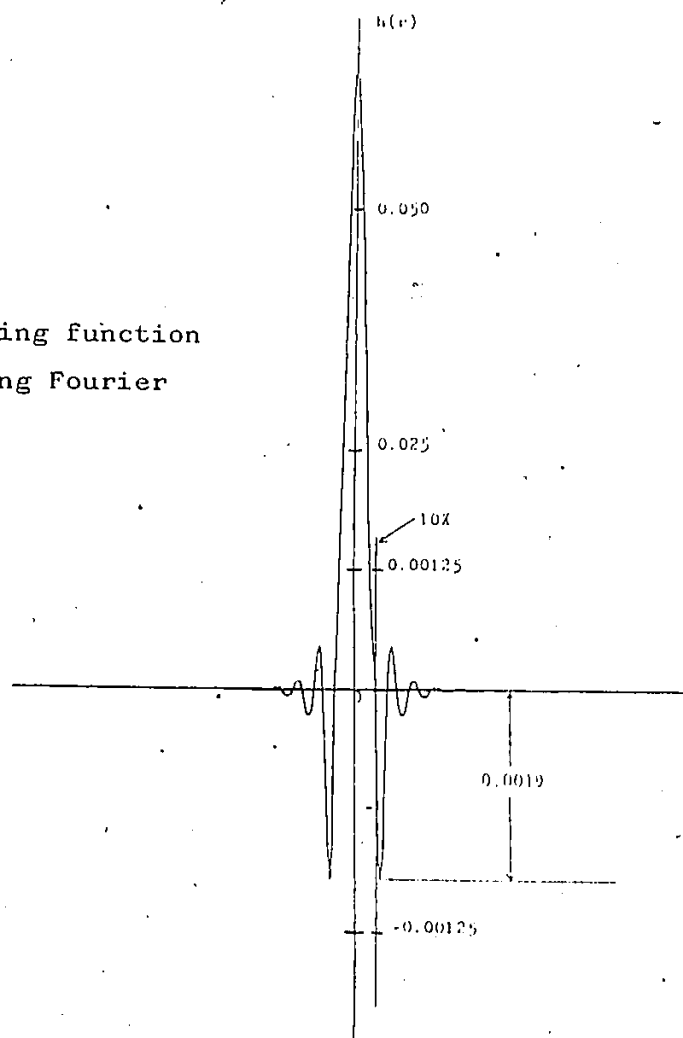


Figure IV-7
Hanning truncating function
and corresponding Fourier
transform



iii) Normalization

The experimental interference curve $I(s)$ is obtained in arbitrary units, the problem is to determine $i(s)$ in absolute units.

Recall equation (71) which stated

$$I(s) = Nf^2(s) \left[1 + \frac{2}{s} \int_0^{\infty} r[\rho(r) - \rho_0] \sin 2\pi s r dr \right]$$

The integral in this equation extends over a short interval since we can expect $[\rho(r) - \rho_0]$ to approach zero at distances of a few atomic diameters. By dividing the r -axis into small intervals δ we can replace the integral by a sum

$$\frac{I(s)}{N} = f^2 + f^2 \sum_i Y_i \frac{\sin 2\pi s r_i}{2\pi s r_i} \quad (89)$$

$$\text{where } Y_i = \int_{r_i - \delta/2}^{r_i + \delta/2} 4\pi r^2 [\rho(r) - \rho_0] dr$$

The variation of $\frac{I(s)}{N}$ above f^2 is

$$\frac{I(s)}{N} - f^2(s) = f^2(s) \sum_i Y_i \frac{\sin 2\pi s r_i}{2\pi s r_i} \quad (90)$$

From this equation we can see that $I(s)/N$ oscillates about f^2 with decreasing amplitude of oscillations, due to the decrease in f^2 and the decrease in the values of $\text{sinc}(2\pi s r_i)$, see figure IV-8.

The units of the f^2 curve are known. In order to obtain $I(s)/N$ in absolute units it is necessary only to multiply the experimental interference function by a suitable factor so that

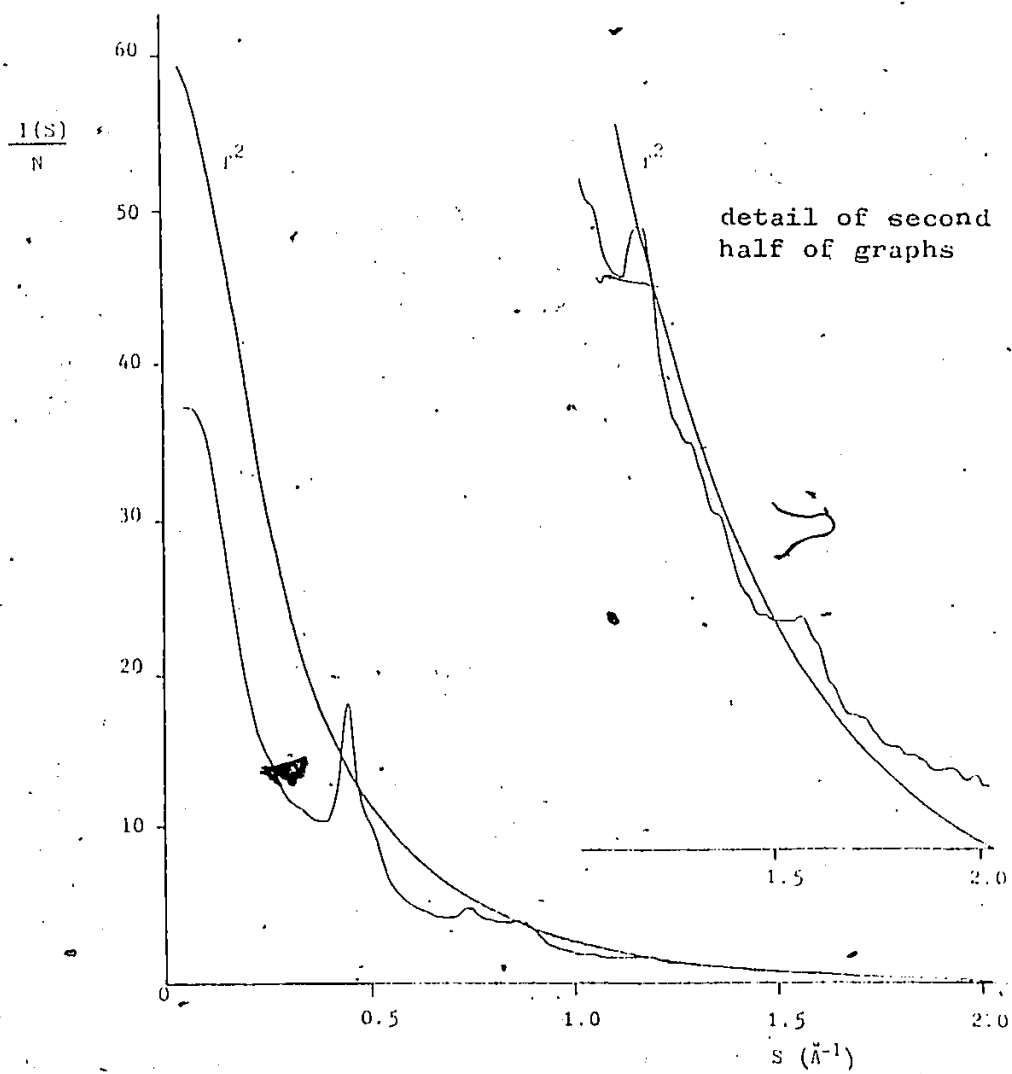


Figure IV-8

$I(s)/N$ and $f^2(s)$ curves for typical sample
 Note the oscillations of $I(s)/N$ about $f^2(s)$

at large s , it oscillates about the $f^2(s)$ curve. Thus we have

$$\frac{I(s)}{N} = I \exp(s) K \quad (91)$$

where K is the normalization constant.

Consider now the effects that would be introduced in the reduced radial function, $G(r)$, as the result of an erroneous normalization constant. Recall that

$$i(s) = s \left[\frac{I \exp K}{f^2(s)} - 1 \right]$$

and

$$G(r) = 8\pi \int_0^\infty i(s) \sin 2\pi s r ds$$

the error introduced in $i(s)$ is

$$\begin{aligned} \Delta i(s) &= \frac{\delta i}{\delta K} \Delta K \\ &= \frac{s I(s)}{f^2} \frac{\Delta K}{K} = \frac{\Delta K}{K} i(s) + \frac{\Delta K}{K} s \end{aligned} \quad (92)$$

the error in $G(r)$ is

$$\begin{aligned} \Delta G &= \frac{\delta G}{\delta K} \Delta K \\ &= \Delta K \cdot 8\pi \int_0^\infty \frac{\delta i(s)}{\delta K} \sin 2\pi s r ds \\ &= \frac{\Delta K}{K} \cdot 8\pi \left[\int_0^\infty i(s) \sin 2\pi s r ds + \int_0^\infty s \sin(2\pi s r) ds \right] \\ \Delta G &= \frac{\Delta K}{K} \left[G(r) + 8\pi \left[\frac{\sin 2\pi s_m r}{4\pi^2 r^2} - \frac{s_m \cos 2\pi s_m r}{2\pi r} \right] \right] \end{aligned} \quad (93)$$

where s_m is the maximum value of s .

The resulting $G(r)$ is composed of two parts, the first is

a true function modified by a change of scale and the second is the transform of a straight line of slope $\Delta K/K$. Kaplow et.al⁽³²⁾ have illustrated these effects and they show that the introduction of a variation as small as one percent from the correct normalization constant produces sharp oscillations in the reduced radial distribution function at values of r close to zero.

This fact can be a useful criterion for the determination of the correct value of the normalization constant. Thus K is chosen as the value that produces the smallest oscillations in $G(r)$ at values close to zero.

So far we have assumed that the scattering factors, $f^2(s)$, were completely accurate. In reality this is not necessarily the case. Due to approximations used in their calculations we can expect the $f^2(s)$ curves to contain some small systematic error. The probable form of this error is

$$\Delta \left[\frac{I}{Nf^2} \right] = \frac{I}{Nf^2} \epsilon(s) \quad (94)$$

where $\epsilon(s)$ is a slowly varying function of s . The resulting error in $i(s)$ is

$$\Delta i(s) = \epsilon i(s) + \epsilon s \quad (95)$$

Combining this with the error caused by choosing an erroneous normalization constant we obtain

$$\begin{aligned} \Delta i(s) &= \left(\epsilon + \frac{\Delta K}{K} \right) \frac{sI(s)}{f^2} \\ \Delta i(s) &= \left(\epsilon + \frac{\Delta K}{K} \right) i(s) + \left(\epsilon + \frac{\Delta K}{K} \right) s \end{aligned} \quad (96)$$

The effect of this error on the reduced radial distribu-

tion function is similar to those described above. The error in $G(r)$ produced by the first term in equation (96) is the convolution of the transform of $(\epsilon + \Delta K/K)$ with the true $G(r)$. Since $(\epsilon + \Delta K/K)$ is a slowly varying function the effect of the convolution is that of a change in scale. The second term $(\epsilon + \Delta K/K)s$ produces sharp oscillations in the region between zero and the first real peak in the reduced radial distribution function. The standard correction procedure used to minimize the effects produced by these errors was developed by Kaplow⁽³²⁾ and will be briefly described here. Consider the reduced radial distribution function, $G(r)$ in the region before the first peak. This peak corresponds to the first nearest neighbour. Now we know that the value of $\rho(r)$ before the first peak is zero. Thus in this region $G(r) = -4\pi r \rho_0$ hence we can think of the errors in this region as modulations about a straight line. Considering again the small region of r between zero and the first peak we may define a function ΔG which is the difference between the experimentally obtained reduced radial distribution function containing the errors, and a straight line $G(r) = -Dr$. Since only the small r region is being considered, the transform of ΔG will correspond to the second term of equation (96) " $(\epsilon + \Delta K/K)s$ " and then Δi can be calculated by multiplying by $I(s)/f^2$. The variable parameter for this procedure is the slope D , the criterion for choosing it is that the error transform $s(\epsilon + \Delta K/K)$ should not contain sharp oscillations near zero.

iv) Non-elastic Collisions

The effect of non-elastic collisions is to increase the scattering background on the diffraction pattern, hence decreas-

ing the measurable intensity of the observable peaks. The two main factors that have to be controlled to minimize the background are the substrate and sample thickness. Due to the non crystalline nature of the formvar substrate its contribution to the diffraction pattern is that of extremely broad peaks of very low intensity. Thus it is desirable to keep the formvar thickness to a minimum so that its contribution is also small. The thickness of the sample should also be kept small to minimize any multiple scattering that might occur. The errors introduced by the background were additive in nature similar to those described by Graczyk et.al.⁽³³⁾. More specifically they have the form

$$i(s) = s \left[\frac{I(s) + \epsilon}{f^2} - 1 \right]$$

where ϵ is a slowly varying function. This type of error is easily detected and corrected. Its main effect is to make $i(s)$ oscillate about a slowly varying function ϵ . To correct we just subtract ϵ so that $i(s)$ properly oscillates about zero.

Chapter V

Results and Discussion

In figure V-1 we present a series of electron micrographs of thin Ni-P grown at different pH values of the metallizing bath (from pH about 8 through pH about 12). Care was taken so that each film was grown approximately to the same thickness. Based on the temperature and pH of the metallizing bath and the time of deposition of each film we estimate the thickness of the films to be of the order of 500 Angstroms. The electron micrographs show the usual picture of a discontinuous film consisting of individual islands. These islands are the result of Sn-Pd nucleation centers present on the surface after activation before metallizing started⁽⁶⁾. We note that as the pH value increases the metal islands are larger and more sparsely distributed on the surface. Also in this connection we observe that each film has nearly uniform island sizes. We attribute this to the following. First, the effect of raising the pH on the hypophosphite is to increase its reduction potential⁽⁵⁾, thus the enhanced film growth rate. Second, it has been observed⁽⁵⁾ that some time in the alkaline bath is necessary before the material present on the substrate after the Sn-Pd sensitization-activation is capable of catalyzing plating. This is expected to result in fewer active nucleation centers available for higher pHs, simply because the time spent in the metallizing bath is shorter.

The tentative models for the Ni-P alloys grown in alkaline environment are those of a solid solution of phosphorus in crystalline fcc nickel structure⁽⁶⁾. Hence as far as this point is concerned a high concentration of phosphorus would result in

Figure V-1 Transmission electron micrographs of electrolessly deposited Ni-P from an alkaline solution grown at different pH values

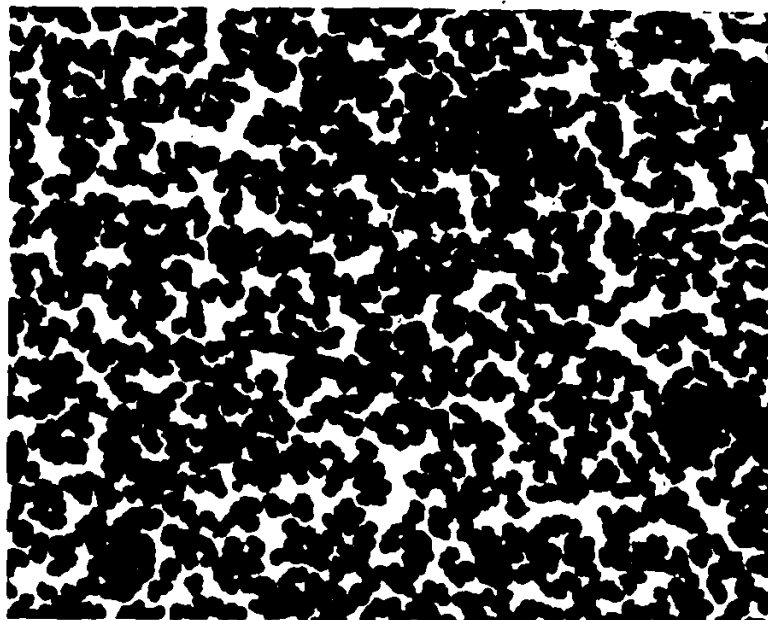


Figure V-1a pH 12.3

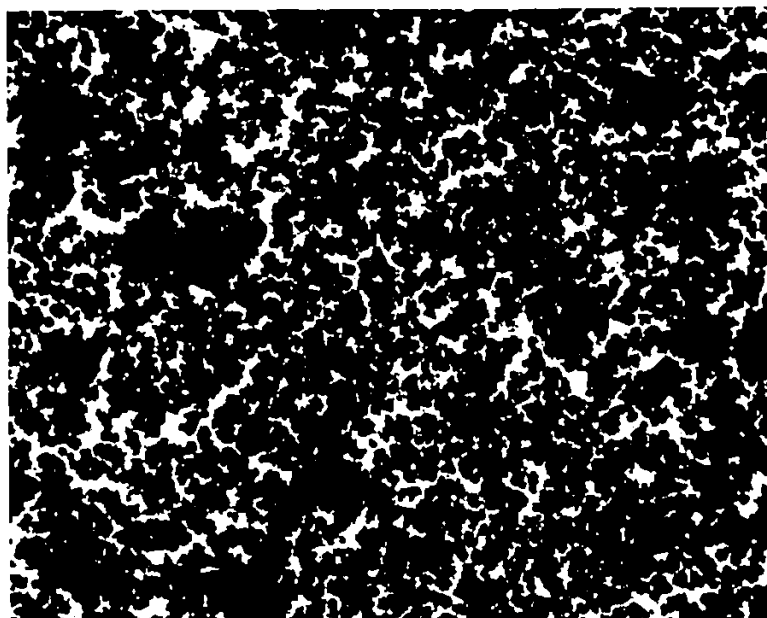


Figure V-1b pH 10.8

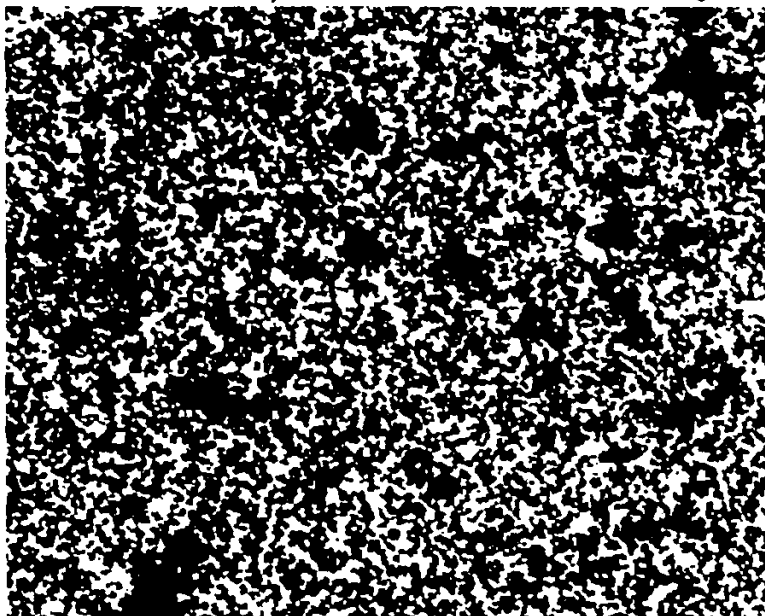


Figure V-1c pH 9.9

↓

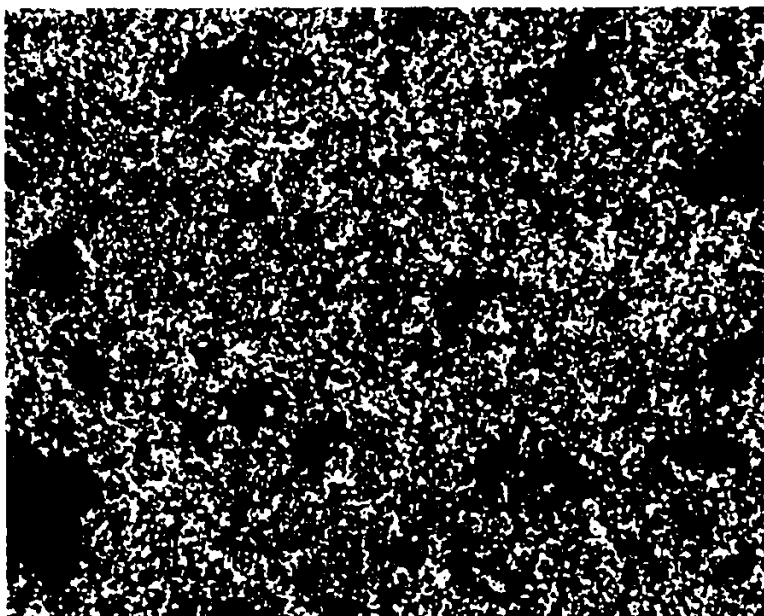


Figure V-1d pH 9.0

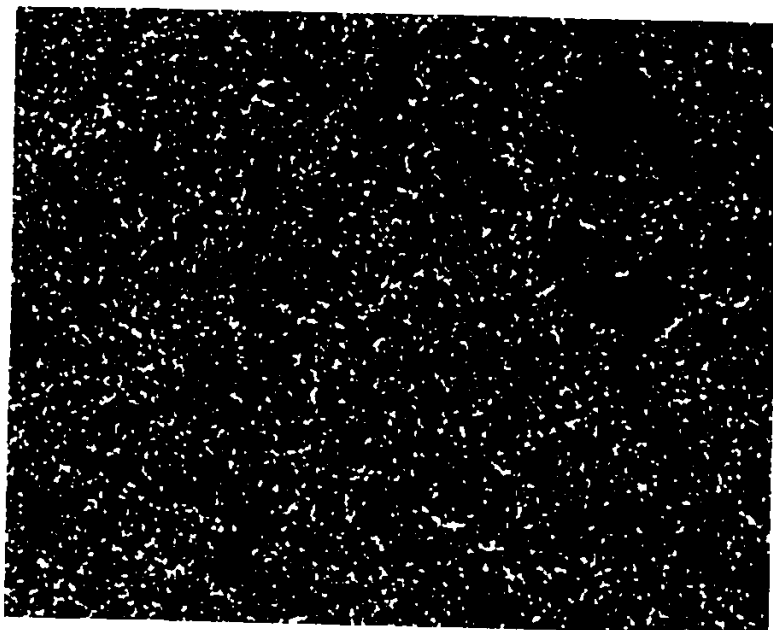


Figure V-1e pH 7.9

~

films was estimated using Energy Dispersive X-ray Analysis as follows. First using as standard a Ni-P film grown in acidic environment with a known phosphorus content was examined. From this measurement the minimum amount of phosphorus that could be detected using this technique was determined to be about 2%. Consequent examination of the films used for the present study showed that no phosphorus could be detected. Hence we conclude that the phosphorus content of all films used was less than 2%.

Figure V-2 presents the densitometer output curves, before smoothing, of the diffraction patterns obtained from the films corresponding to figure V-1

The broadening of the peaks of the diffraction pattern can be initially attributed to one or more of the following:

- i) Partial crystallinity
- ii) Small crystallite sizes
- iii) Internal strains

The effects of large stresses and strains on the lattice are easily recognizable, for they tend to broaden the diffraction peak in the direction of the stress or strain, far more than any of the other peaks. This effect is not observed on the series of diffraction patterns presented in figure V-2, thus whatever stresses and strains are acting on these films are not dependent on the pH of the metallizing bath. The observable broadening of the peaks is relatively smooth as the pH increases, this suggests that the broadening is mainly due to changes in the crystallite sizes.

It is known⁽³⁵⁾ that the size contribution to the width of the Bragg diffraction peak Δs is related to the crystallite

Figure V-2 Diffraction pattern curves corresponding to films
shown in figure V-1

(A) pH = 12.3

(B) pH = 10.8

(C) pH = 9.9

(D) pH = 9.0

(E) pH = 7.9

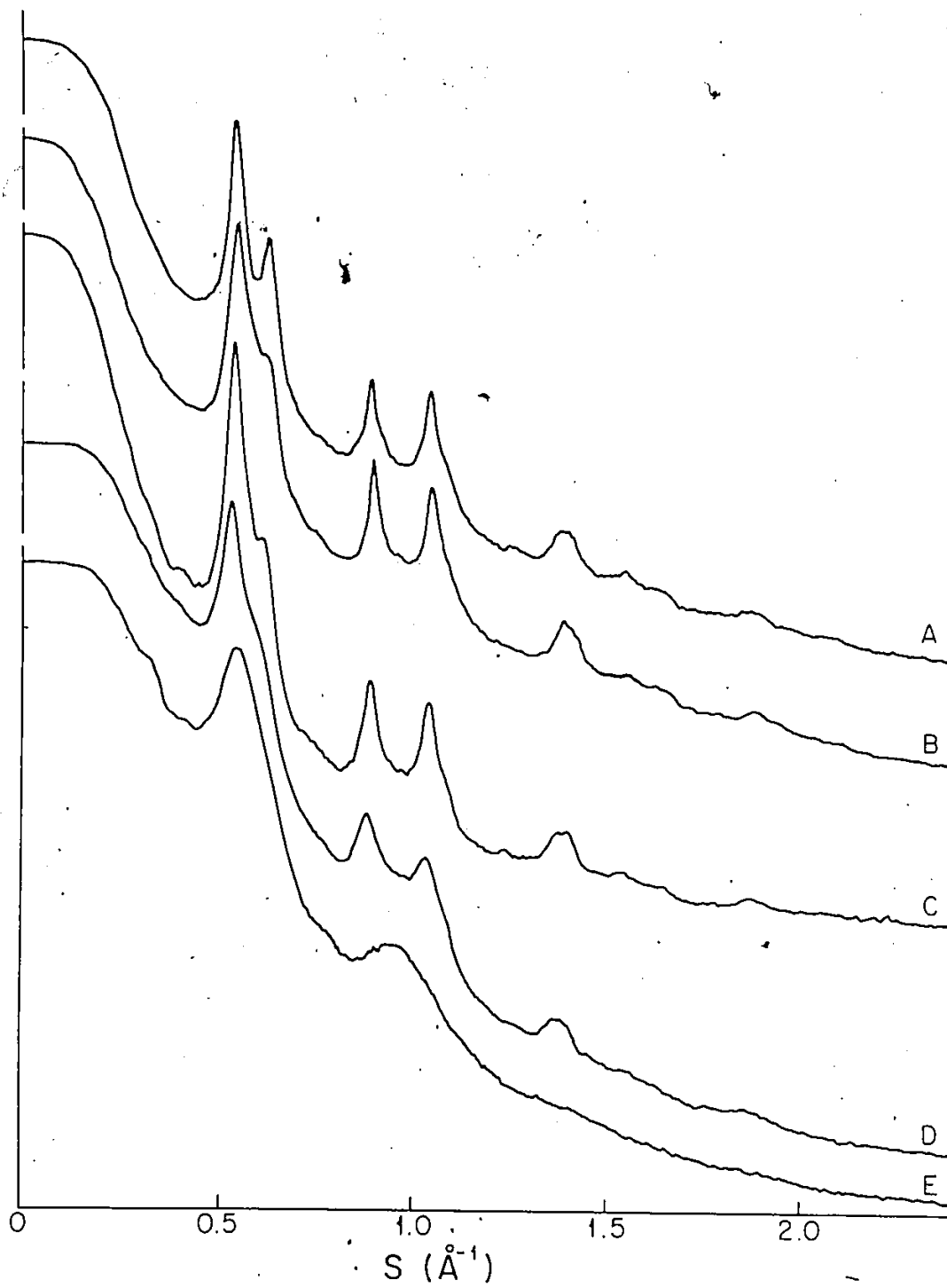


Figure V-2

sizes, D , normal to the diffraction plane by the expression

$$\Delta = C/D \quad (97)$$

where C is a quantity which depends on the Miller indices of reflection and the shape of the crystallite. For isotropic crystallites however it is about unity for all reflections. As the sizes of the crystallites decreases all peaks are expected to broaden. This can be observed to be the case in figure V-2. The crystallite sizes as determined by equation (97) are given in table V-1. The island sizes are determined from figure V-1 are given as approximate ranges between the smallest and largest island observed in each sample.

pH	island sizes (A)	Crystallites sizes (Angstroms)		
		111	220	311
12.3	600-700	22	32	32
10.8	400-600	--	26	28
9.9	300-400	17	21	26
9.0	200-300	15	17	24
7.9	100-200	11	--	--

-- peaks not clearly resolved

Table V-1 Island and crystallite sizes

Figures V-3 and V-4 give the $i(s)$ curves obtained after the correction procedure. From these the reduced radial distribution functions, $G(r)$, were calculated.

It is important to realize that the information that the reduced RDF provides is inherently present in the diffraction pattern; the reduced RDF just gives us this information in a way that is simpler to examine. The $G(r)$ curves show average one

Figures V-3, V-4 $i(s)$ curves obtained after correction
procedures

Figure V-5, V-6 Reduced RDF ($G(r)$) curves corresponding to
curves (A) - (D) in figure V-2

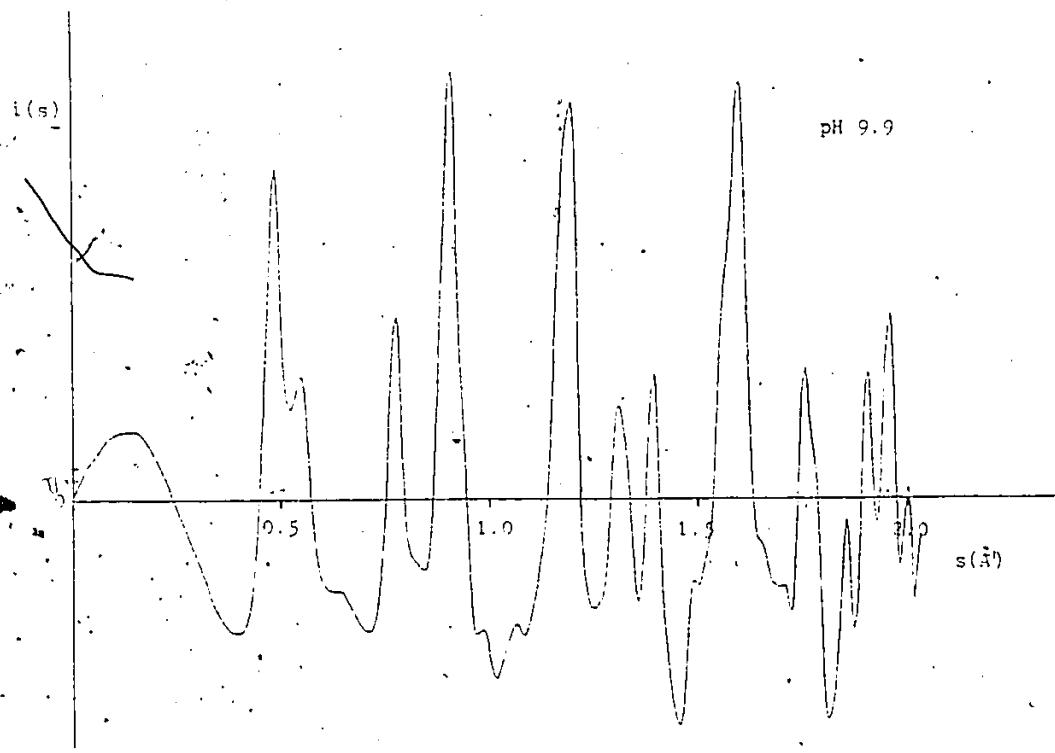
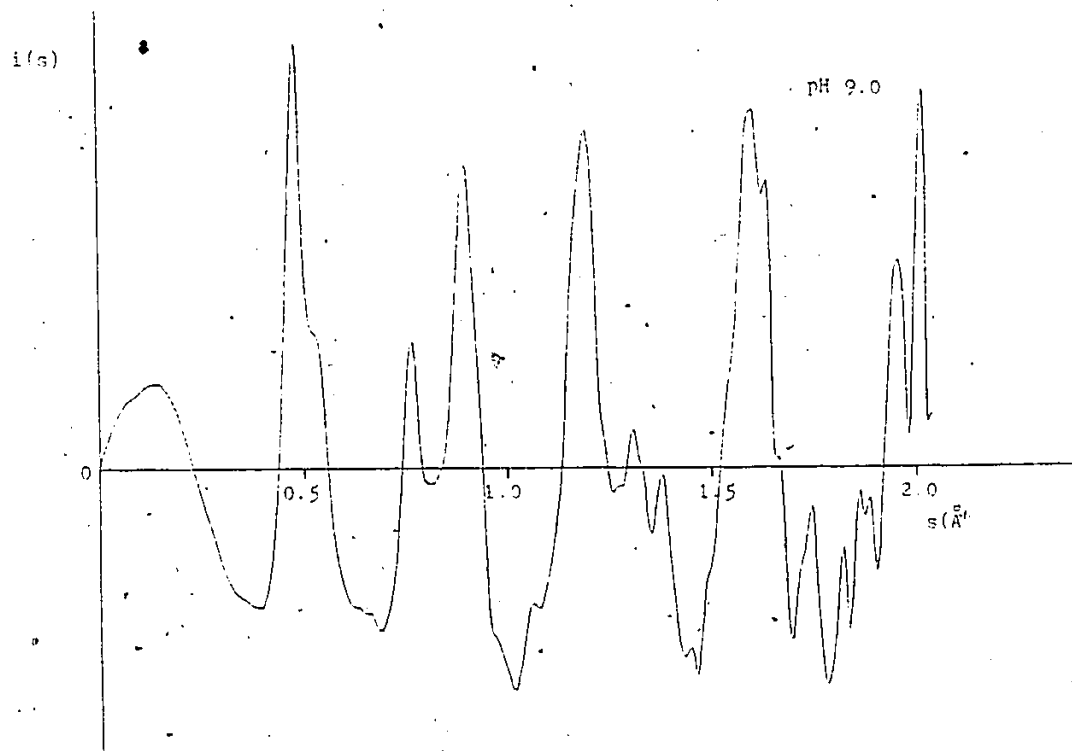


Figure V-3

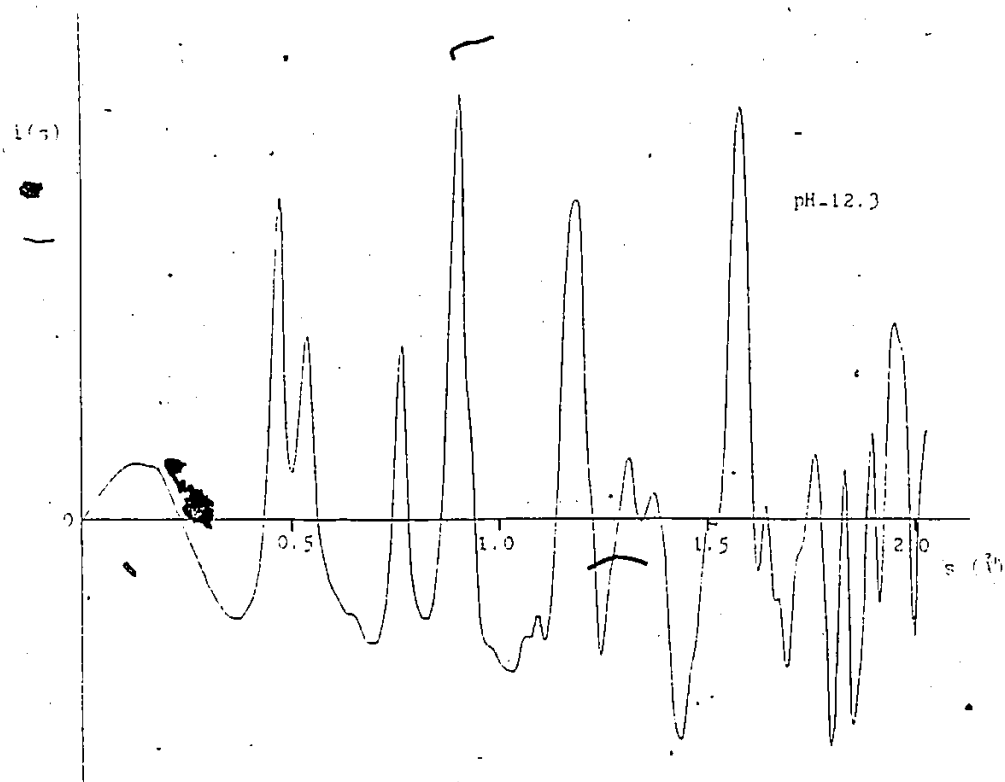
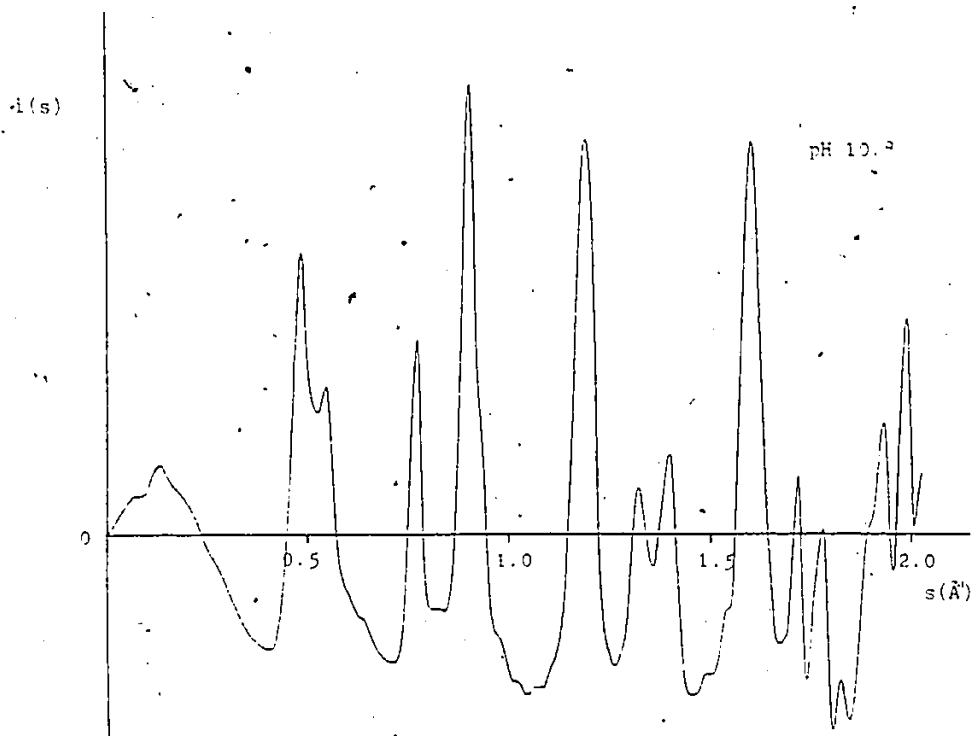


Figure V-4

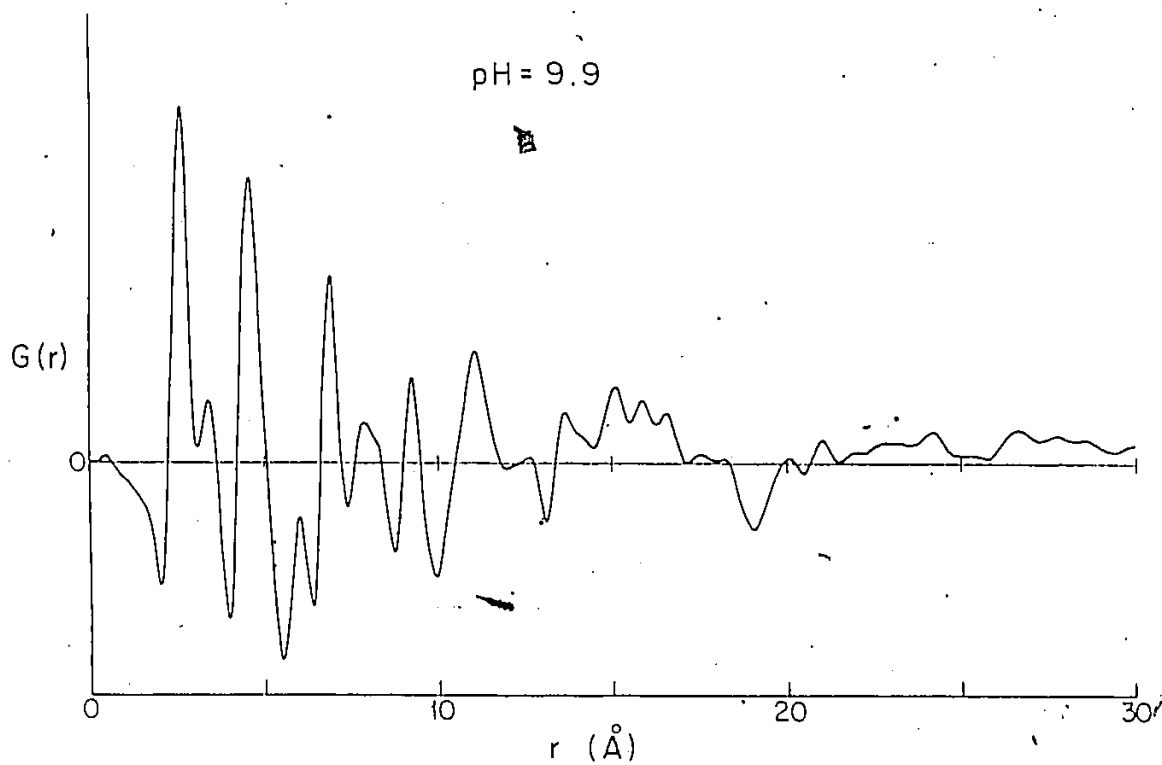
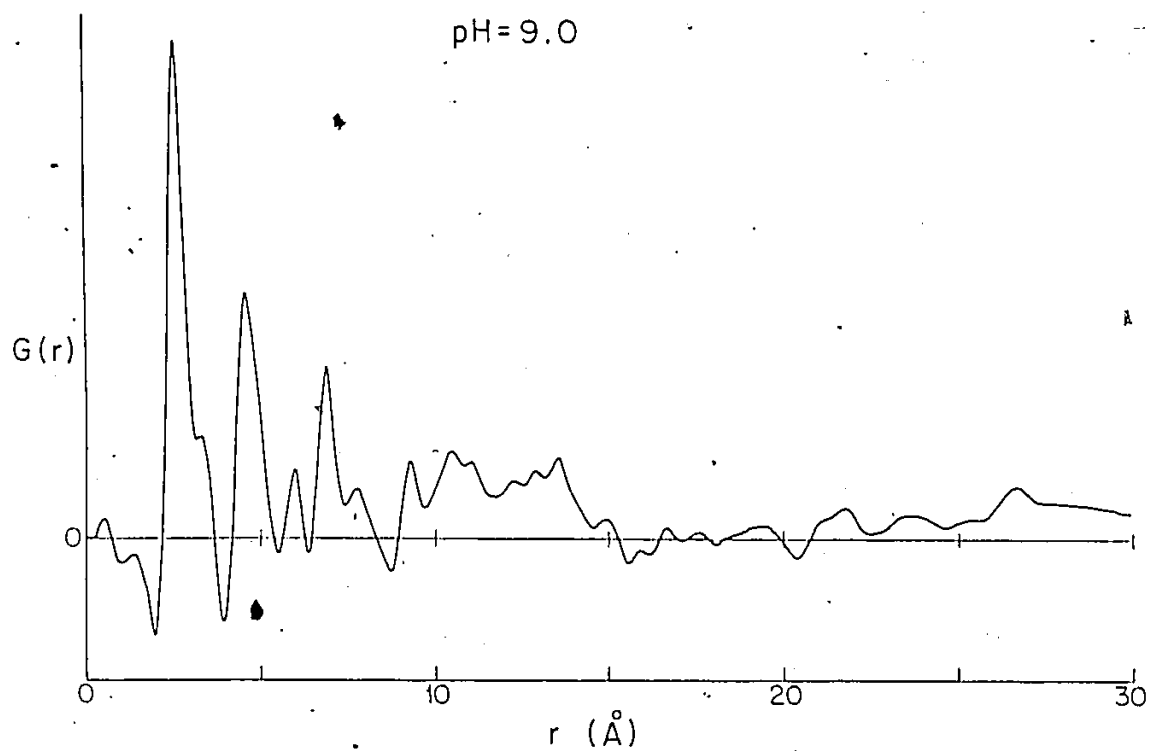


Figure V-5

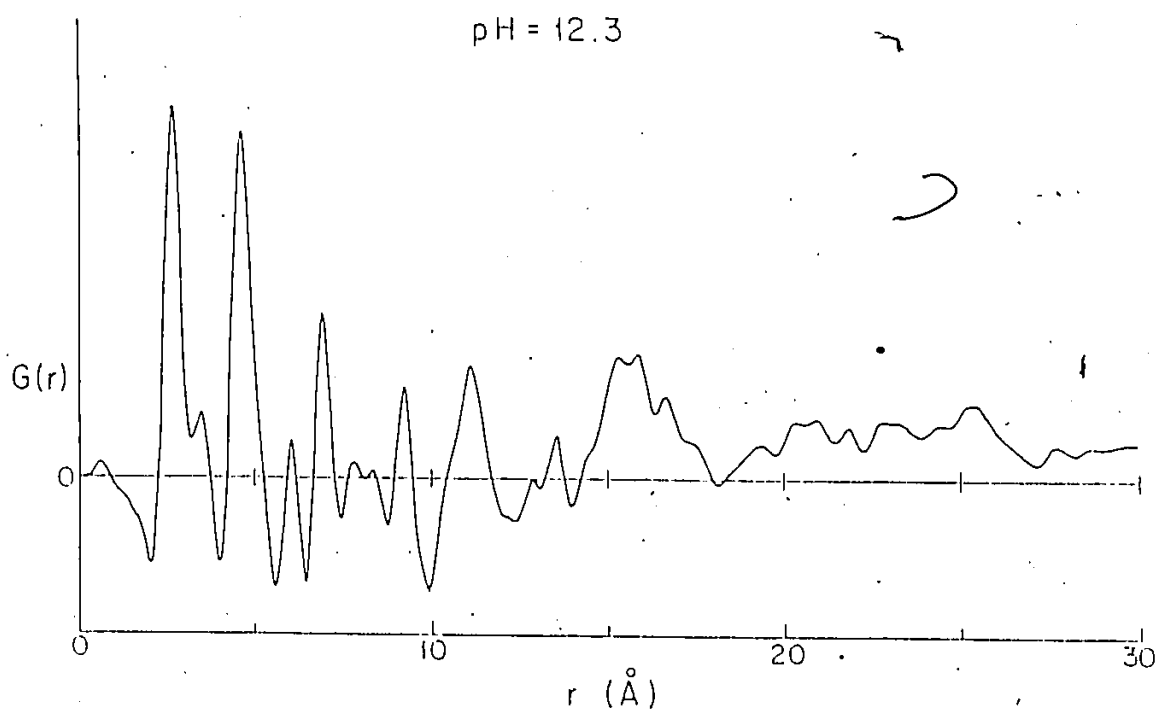
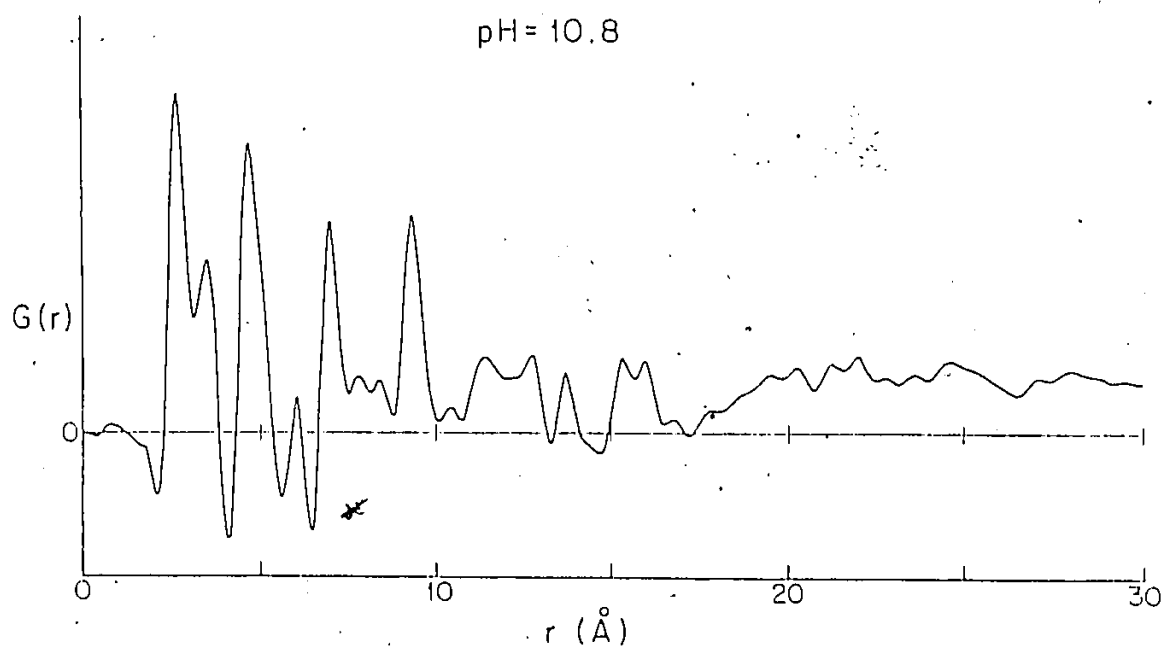


Figure V-6

dimensional information about the locally varying three dimensional structure of the thin films. For a crystalline material the reduced RDF would contain sharp peaks corresponding to the various distances of each neighbour. For example if the sample being studied had fcc structure, then the reduced RDF would show a sharp neighbour peak follow by peaks at distances $\sqrt{2}$, $\sqrt{3}$, 2, etc. relative to the first peak distance. As the crystallinity of the sample decreases we can expect the following changes in the reduced RDF. Generally all the peaks will become broader, some of them might shift position and if the amorphicity is high enough some of the peaks will disappear. Figure V-5 and V-6 gives the reduced RDF curves obtained from the samples shown in figure V-1, the reduced RDF corresponding to the film grown at pH 7.9 was not calculated since we felt that its phosphorus content would not be low enough to justify the single species treatment used for the rest of the samples. Table V-2 presents the location of the first ten peaks in each of the reduced RDF curves.

pH	distance r corresponding to 10 first peaks (angstroms)									
	1	2	3	4	5	6	7	8	9	10
12.3	2.6	3.5	4.6	6.0	6.9	7.7	8.2	9.1	10.4	11.0
10.8	2.6	3.5	4.6	6.0	6.9	7.7	8.3	9.2	10.3	11.2
9.9	2.6	3.4	4.6	6.0	6.9	7.8	8.2	9.2	-	11.0
9.0	2.6	3.3	4.6	6.0	6.9	7.7	-	9.2	10.4	11.0

Table V-2 First ten peak locations in $G(r)$ curves

The reduced RDF curves lead to the following observations. Each curve could be thought of being composed of three regions, a region of sharp well defined peaks corresponding to

short range order, a region of small broad peaks corresponding to the long range order and a small transition region separating the two. From table V-2 we observe that within the region of short order the position of the peaks does not vary as the pH changes, on the other hand the relative intensities of some peaks does change and we also observe that as the pH increases the peaks become better resolved.

From the above observations a consistent model for the structure of our films can be offered. The general feature of earlier models^(6,36) is retained, namely that with increasing pH of the metallizing bath, i.e. decreasing phosphorus content we can expect the films to be more crystalline. The present work however clarifies and finalizes the model. The islands, whose origin is traceable to the nucleation centers^(6,37), are made up of component crystallites whose dimensions are strongly pH dependent. The dependence is such that we observe a doubling of the crystallites size as the pH is increased from 8 to 12. We further observe that the short range order as deduced from the reduced RDF curves also increases with pH, as a matter of fact it would seem that the extend of the short range order nearly equals the crystallite sizes. In this model a few points require further work, but some speculative considerations may be given. Consider the varying relative intensities of some of the peaks in the reduced RDF curves. First of all we should point out that the area under each peak is a measure of the number of atoms that are located at the distance marked by the peak. This area under the peaks is commonly referred to as the coordination number. Previous work⁽³⁸⁾ has

shown that the as deposited Ni-P films have a lower material density than that of bulk nickel. This fact might explain the changes in the intensities if we assume that the films obtain their lower density by having consistently vacant sites. Another and not unrelated possibility is that some regularly distributed sites are occupied by the phosphorus atoms. In practice we might expect that the real situation is a combination of the two given explanations.

Another point is the difference between the nearest neighbour distance in bulk nickel, 2.5 angstroms, and the value obtained for our films, 2.6 angstroms. Here we might draw a parallel to the comparative study of solid aluminum and aluminum at the melting point carried out by the MIT group⁽³⁹⁾. In their studies the differences between the reduced RDF curves for solid and liquid aluminum were possible to explain assuming a quasi-crystalline model in which the reduced RDF of the solid is broadened and damped by the introduction of a definite crystallite size and liquid diffusive motions. In our films we not only have small crystallites but an aggregate of these form small islands. Thus, not as in a solid a given atom sees an interrupted periodic potential; the atoms in our films will "feel" the influence of the physical boundaries of the crystallites and islands that interrupt the periodicity. In conclusion our model for the electroless Ni-P films grown in alkaline solution consists of highly ordered component crystallites of very small size which are strongly affected by the relative large surface to volume ratio of the crystallites and islands, giving us the liquid like appearance of the reduced RDF.

Appendix 1

Computer Implementation

The configuration of the computer system used for the implementation of the techniques described in the text is as follows:

CPU - LSI 11

Memory - 32 Kwords

Video Terminal - VT55 with graphics resolution of 512x236 pixels

Line Printer - LA 120, 120 characters per second

Storage - 2 RK05 hard disk drives with 2.5 MBytes/disk

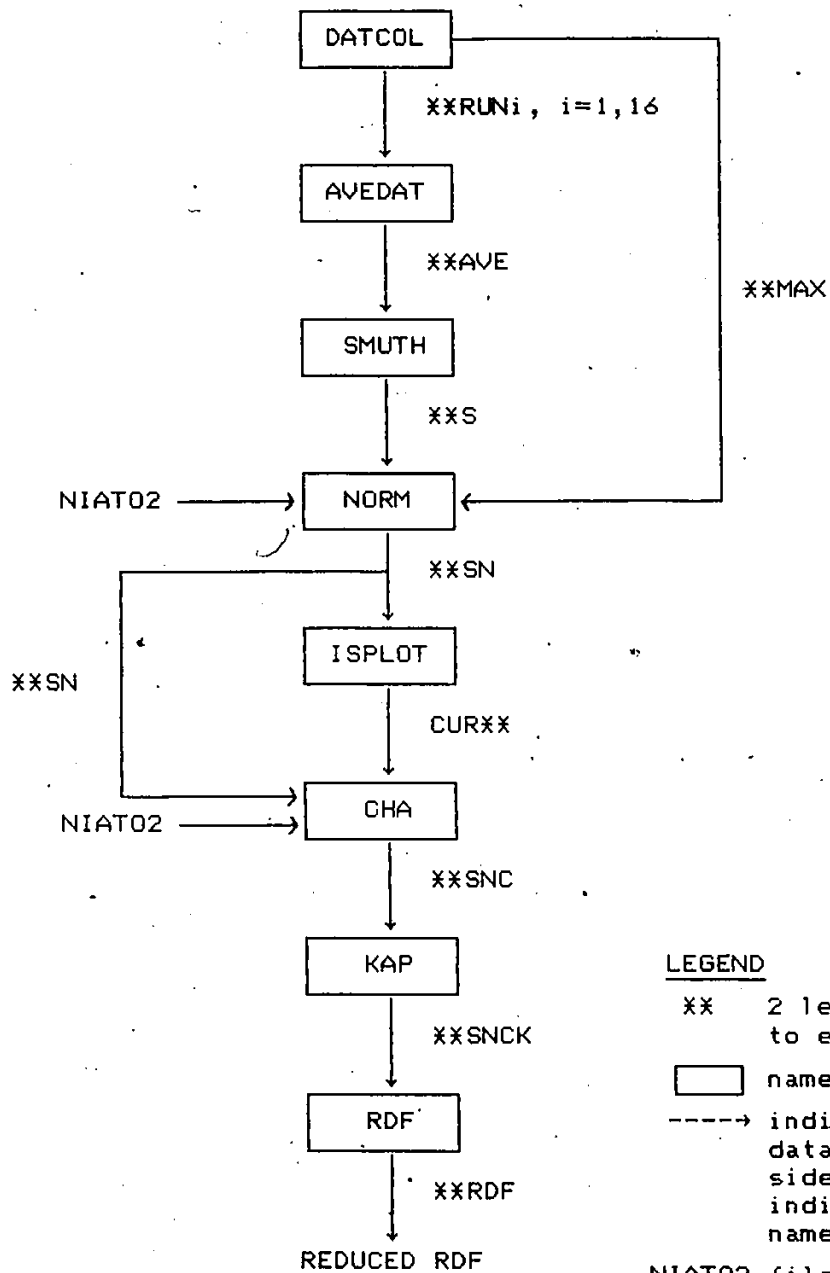
Extras - A/D, D/A converters and programmable clock

The programs developed for the acquisition and correction of the data were designed to give the user maximum flexibility fully utilizing the available hardware. Each program represents a logical step towards the calculation of the reduced RDF, and the results of each step are permanently stored in a disk as a file. Hence if for any reasons one of the steps fails not all the previous work is lost. Also whenever possible the programs were of an interactive nature, i.e. the programs would inquire whether the last data manipulation was satisfactory and if not, it would allow the user to repeat the step.

At the heart of the calculations lies the Fast Fourier Transform, the algorithm used to implement it was the Sande-Tuckey⁽³⁹⁾ as given by Monro^(40,41).

A step by step chart illustrating the calculation of the reduced RDF is given here together with the names of the input and output files used during the process.

Appendix 1



LEGEND

XX 2 letter code assigned to each sample

name of subprogram

-----> indicates flow of data, the name beside the arrows indicates the file name

NIAT02 file containing square of atomic scattering factors for Ni

Appendix 2
Program Listings

```

CXXXXXXXXXXXXXXXXXXXXXXXXXXXXXXXXXXXXXXXXXXXXXXXXXXXXXXXXXXXX
C
      PROGRAM DATCOL
C
C      CALLER PROGRAM TO COLLECTS NEW DATA FROM DENSITOMETER
C      OR READ DATA FROM A ALREADY CREATED FILE.
C      USES THE OFFSET FEATURE TO DETERMINE THE MIDDLE POINT
C
CXXXXXXXXXXXXXXXXXXXXXXXXXXXXXXXXXXXXXXXXXXXXXXXXXXXXXXXXXXXX
      REAL ARRAY1(520),ARRAY2(520),ARRAY3(520)
      INTEGER BUF(30),N1(1100),RIGHT(520),LEFT(520)
      EQUIVALENCE(ARRAY1(1),RIGHT(1))
      INTEGER OFFSET
      LOGICAL X1 IANS
      REAL X8 IDNA
200      FORMAT(A6)
58      FORMAT(7I7)
333      FORMAT(17)
C
C      INITIALIZE
C
      N=512
      M=2XN
      NMAX=1100
      DO 77 I=1,38
77      BUF(I)=0
      PI=3.1415926
      FLAG=0
C
C      THE USER CAN EITHER CREATE A FILE WITH NEW DATA
C      OR EXAMINE AN OLD DATA FILE
C
1      CALL CLEPLT
      TYPE X,'READ OR WRITE?(R or W)'
      CALL INCHAR(IANS)          !READ CHARACTER FROM KEYBOARD
      IF(IANS.EQ.'R') GO TO 2
      IF(IANS.NE.'W') GO TO 1
      GO TO 3
C
C      CODE FOR CREATING FILE WITH NEW DATA
C
2      FLAG=1
3      CALL CLEAR
      TYPE X,'FILE NAME?'
      READ(7,200) IDNA
      CALL ASSIGN(20,IDNA)
      IF(FLAG.EQ.1) GO TO 90
      TYPE X,'TAKING IN DATA'
      TYPE X,
      CALL INDATA(N1,NMAX,11)    !COLLECT THE DATA FROM DENSITOMETER
      WRITE(20,58) NMAX
      WRITE(20,58) (N1(I),I=1,NMAX)
      GO TO 38
C
C      CODE TO EXAMINE OLD DATA FILE
C
90      READ(20,58) NUMPTS
      READ(20,58) (N1(I),I=1,NUMPTS)

```



```

30  CALL CLOSE(20)
    CALL BELL                                !RINGS BELL TO WARN THAT RUN IS OVER
C
C  THE DATA ACQUIRED REPRESENTS THE DOUBLE SIDED DIFFRACTION PATTERN
C  IN THE FOLLOWING CODE THE USER INTERACTIVELY USING THE SYMMETRY
C  OF THE DIFFRACTION PATTERN FINDS THE MIDDLE POINT
C
    OFFSET=0
    GO TO 42
445  CALL CLEPLT
    TYPE X,'OFFSET?'
    READ(7,333) OFFSET
42   CALL MOVE(N1,NMAX,OFFSET,RIGHT,LEFT)  !FINDS MIDDLE POINT ACCORDING
                                           !TO OFFSET GIVEN BY USER
    DO 33 J=1,N
    ARRAY3(J)=RIGHT(J)
33   ARRAY2(J)=LEFT(J)
    CALL PLTSM(ARRAY3,ARRAY2,N,0) !DISPLAYS RIGHT & LEFT SIDE IN SCREEN
443  CALL CLEPLT
    TYPE X,'SATISFIED?(Y OR N)'
    CALL INCHAR(IANS)
    IF(IANS.EQ.'N') GO TO 445
    IF(IANS.NE.'Y') GO TO 443
5    CALL CLEAR
C
C  ONCE THE MIDDLE POINTS IS DETERMINED THE USER HAS THE CHOICE TO
C  1)AVERAGE THE LEFT AND RIGHT SIDE
C  2)SAVE IN A FILE THE LEFT, RIGHT OR AVERAGE SINGLE SIDED PATTERNS
C
    TYPE X,'DO YOU WISH TO AVERAGE? (Y OR N)'
    CALL INCHAR(IANS)
    IF(IANS.EQ.'N') GO TO 999
    IF(IANS.NE.'Y') GO TO 5
    CALL AVERAG(RIGHT,LEFT,N)              !AVERAGES LEFT AND RIGHT SIDES
    DO 34 J=1,N
34   ARRAY2(J)=RIGHT(J)
    CALL PLOT(ARRAY2,N)
999  CALL CLEPLT
    TYPE X,'DO YOU WISH TO SAVE? (Y OR N)'
    CALL INCHAR(IANS)
    IF(IANS.EQ.'Y') GO TO 35
    IF(IANS.NE.'N') GO TO 999
    GO TO 998
35   CALL CLEAR
    TYPE X,'WHICH SIDE?(L , R , A)'
    CALL INCHAR(IANS)
    IF(IANS.EQ.'A') GO TO 548
    IF(IANS.EQ.'L') GO TO 555
    IF(IANS.NE.'R') GO TO 35
    GO TO 548
555  ILFLG=1
548  CALL CLEAR
C
C  USER CAN SPECIFY THE NAME OF THE FILE BEEN CREATED
C
    TYPE X,'FILE NAME?'
    READ(7,200) IDNA
    CALL ASSIGN (21,IDNA)
    IF(ILFLG.EQ.1) GO TO 544

```

```

WRITE(21,58)(RIGHT(I),I=1,N)
GO TO 549
544 WRITE(21,58)(LEFT(I),I=1,N)
GO TO 549
549 CALL CLOSE(21)
998 CALL CLEPLT
CALL EXIT
END

```

```

;XXXXXXXXXXXXXXXXXXXXXXXXXXXXXXXXXXXXXXXXXXXXXXXXXXXXXXXXXXXX

```

```

; ROUTINE INDATA.

```

```

; THIS ROUTINE OBTAINS DATA POINTS THROUGH THE ADC
; EACH FINAL POINT IS THE AVERAGE OF 8 CONSECUTIVE
; SAMPLED POINTS.

```

```

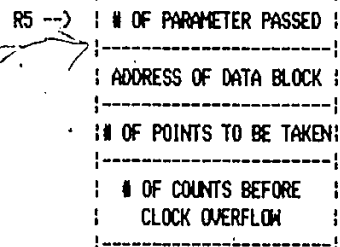
; CALLER PROGRAM: DATCOL

```

```

; THE LINKAGE OF THIS ROUTINE IS DONE AS FOLLOWS:

```



```

; FOR DETAILS OF ADC OPERATION SEE:
; ADV11-A,KW11-A,AAV11-A,DRV11 USER'S MANUAL

```

```

;XXXXXXXXXXXXXXXXXXXXXXXXXXXXXXXXXXXXXXXXXXXXXXXXXXXXXXXXXXXX

```

```

.MCALL .PRINT,.EXIT
.TITLE INDATA
.GLOBL INDATA,CLEAR
.MACRO SAVREG
MOV R0,-(SP)
MOV R1,-(SP)
MOV R2,-(SP)
MOV R3,-(SP)
MOV R4,-(SP)
MOV R5,-(SP)
.ENDM SAVREG

```

```

.MACRO RESREG
MOV (SP)+,R5
MOV (SP)+,R4
MOV (SP)+,R3
MOV (SP)+,R2
MOV (SP)+,R1
MOV (SP)+,R0
.ENDM RESREG

```

```

TTS=177564
TTB=TTT+2
CLKSR=178428
CLKBR=178422

```

```

ADSR=170400
ADDR=170402
INDATA: SAVREG      ;SAVE REGISTERS
MOV    #42,@CLKSR    ;42 FOR 1KHz, 52 FOR 100Hz
MOV    #40,@ADSR     ;SET CLOCK ENABLE
MOV    2(R5),ADDR     ;ADDR <-- ADDRESS OF DATA BLOCK
MOV    @4(R5),R0      ;R0 <-- # OF POINTS TO BE SAMPLED
MOV    @6(R5),R1      ;R1 <-- # OF COUNTS DESIRED BEFORE
                        ;OVERFLOW
NEG     R1             ;TAKE 2'S COMPLIMENTS
MOV     R1,@CLKBR     ;INSERT INTO CLOCK'S BUFFER
CLR     R1             ;
BIC     #200,@ADDR    ;
INC     @CLKSR        ;START SAMPLING
LOOPA: CLR    R3       ;R3 WILL CONTAIN THE AVERAGE OF 8
                        ;POINTS
MOV     #8,R4         ;SET COUNTER
LOOP:   TSTB   @ADSR   ;IS A.D. READY?
BPL     LOOP         ;WAIT UNTIL READY
BIC     #200,@CLKSR   ;
MOV     @ADDR,R2      ;GET SAMPLED POINT
BIT     #100000,@ADSR ;CHECKS FOR DATA LOST
BNE     ERROR        ;
ADD     R2,R3         ;ADDS TO TOTAL
SOB     R4,LOOP      ;GOES BACK UNTIL IT GETS 8 POINTS
CLC     ;CLEAR CARRY BIT
ASR     R3           ;DIVIDE BY 8 TO FIND AVERAGE
ASR     R3           ;
ASR     R3           ;
SUB     #4000,R3     ;SUBTRACT ADC OFFSET
MOV     R3,BADDR     ;STORE POINT IN DATA BLOCK
ADD     #2,ADDR      ;INCREMENT POINTER IN DATA BLOCK
JSR     PC,PRINT     ;SHOW IN SCREEN # OF POINTS SAMPLE
                        ;SO FAR
SOB     R0,LOOPA     ;GOES BACK UNTIL ALL DATA POINTS
                        ;ARE TAKEN
MOV     #0,@CLKSR    ;STOPS CLOCK
FINI:   RESREG      ;RESTORES REGISTERS
RTS     PC           ;RETURNS TO CALLER PROGRAM

```

THIS SECTION WILL TAKE OCTAL NUMBERS AS INPUT
AND PRINT THEIR DECIMAL EQUIVALENT IN THE SCREEN

```

PRINT: SAVREG      ;SAVE REGISTERS
MOV     R0,R5       ;R5 CONTAINS NUMBER TO BE PRINTED
MOV     #DTABL,R2   ;R2 <-- ADDRESS OF TABLE WITH
                        ;POWERS OF 10
MOV     #5,R1       ;R1 <-- # OF DIGITS IN NUMBER
LOOP1:  CLR     R4   ;CLEAR R4 FOR DIVISION
DIV     (R2)+,R4    ;EXTRACT DIGIT
ADD     #60,R4      ;ADD ASCII BIAS
JSR     PC,TYPE     ;PRINT IN SCREEN
SOB     R1,LOOP1    ;GO BACK UNTIL ALL DIGITS ARE DONE
JSR     PC,CR       ;FINISH PRINTING
RESREG      ;RESTORE REGISTERS
RTS     PC         ;RETURN

TYPE:   TSTB   @NTTS ;IS SCREEN READY?
BPL     TYPE   ;WAIT UNTIL READY

```

Appendix 2

```

      MOV    R4,#NTTB      ;PUT DECIMAL NUMBER IN SCREEN
      RTS    PC            ;RETURN

CR:   MOVB   #15,R4        ;PUT CARRIAGE CONTROL CODE --> R4
      JSR    PC,TYPE       ;PRINT IN SCREEN
      RTS    PC            ;RETURN

ERROR: MOV    #0,#CLKSR    ;IN ERROR CONDITION, STOP CLOCK
      .PRINT #FOR          ;AND PRINT SUITABLE MESSAGE
FOR:   .ASCIZ /FLAG OVERRUN SET - SOME DATA LOST/
      .EVEN
      .EXIT

ADDR:  0
FLAG:  0
DTABL: 10000.,1000.,100.,10.,1
      .END

;XXXXXXXXXXXXXXXXXXXXXXXXXXXXXXXXXXXXXXXXXXXXXXXXXXXXXXXXXXXXXXXXXXXX
;
;   ROUTINE AVERAG
;
;   ROUTINE TO AVERAGE TWO INPUT DATA FILE CONTAINING INTEGER DATA
;   THE AVERAGED DATA IS RETURNED IN THE FIRST ARRAY SPECIFIED IN THE
;   DATA LINKAGE
;
;   DATA LINKAGE IS STANDARD (SEE ROUTINE INDATA)
;
;XXXXXXXXXXXXXXXXXXXXXXXXXXXXXXXXXXXXXXXXXXXXXXXXXXXXXXXXXXXXXXXXXXXX
;
;   .TITLE AVERAG
;   .GLOBL AVERAG
AVERAG:
      MOV    R0,-(SP)      ;SAVE REGISTERS
      MOV    R1,-(SP)      ;
      MOV    R2,-(SP)      ;
      MOV    R3,-(SP)      ;
      MOV    R4,-(SP)      ;
      MOV    R5,-(SP)      ;
      MOV    2(R5),R0      ;R0 <-- ADDRESS OF FIRST ARRAY
      MOV    4(R5),R1      ;R1 <-- ADDRESS OF SECOND ARRAY
      MOV    6(R5),R2      ;R2 <-- # OF POINTS IN ARRAYS
LOOP:  MOV    (R1)+,R3      ;R3 <-- POINT OF FIRST ARRAY
      ADD    (R0),R3      ;ADD POINT OF SECOND ARRAY
      CLC                ;CLEAR CARRY BIT
      ASR    R3           ;DIVIDE BY TWO
      MOV    R3,(R0)+     ;STORE RESULT
      SOB    R2,LOOP      ;REPEAT UNTILL DONE
      MOV    (SP)+,R5      ;RESTORE CALLER REGISTERS
      MOV    (SP)+,R4      ;
      MOV    (SP)+,R3      ;
      MOV    (SP)+,R2      ;
      MOV    (SP)+,R1      ;
      MOV    (SP)+,R0      ;
      RTS    PC            ;RETURN
      .END

;XXXXXXXXXXXXXXXXXXXXXXXXXXXXXXXXXXXXXXXXXXXXXXXXXXXXXXXXXXXXXXXXXXXX
;
;   ROUTINE MOVE
;
;   TAKES AN ARRAY OF DATA POINTS AS INPUT AND BREAKS IT
;   INTO A LEFT AND RIGHT ARRAY ACCORDING TO THE OFFSET

```

```

; SPECIFIED IN THE CALLER ROUTINE.
;
; THE LEFT AND RIGHT ARRAYS WILL CONTAIN 512 POINTS EACH.
; THE INPUT DATA USUALLY CONTAINS 1100 POINTS.
;
; THE PROGRAM CHECKS IF THE MIDDLE POINT IS SITUATED IN SUCH POSITION
; THAT EITHER THE LEFT OR RIGHT ARRAY WILL NOT CONTAIN THE FULL 512
; POINTS, AND IF SO IT FILLS THE REMAINING SPACE WITH ZEROS.
;
; CALLER PROGRAM: DATCOL
;
; THE DATA LINKAGE IS STANDARD, (SEE ROUTINE INDATA.MAC)
;
;XXXXXXXXXXXXXXXXXXXXXXXXXXXXXXXXXXXXXXXXXXXXXXXXXXXXXXXXXXXXXXXXXXXX
; .TITLE MOVE
; .GLOBL MOVE
MOVE:
MOV     2(R5),@ARRAY ;ARRAY <-- ADDRESS OF INPUT DATA
MOV     8(R5),@NMAX   ;NMAX <-- # OF DATA POINTS
MOV     8(R5),@OFFSET ;OFFSET
MOV     18(R5),@RIGHT ;RIGHT <-- ADDRESS OF RIGHT ARRAY
MOV     12(R5),@LEFT  ;LEFT <-- ADDRESS OF LEFT ARRAY
MOV     @NMAX,R1      ;R1 <-- # OF POINTS
ASR     R1            ;DIVIDE BY 2
MOV     R1,@HALF      ;STORE IN HALF
MOV     @NMAX,R1      ;R1 <-- # OF POINTS
SUB     #512,R1       ;FINDS UPPER LIMIT
MOV     R1,@HLIM      ;STORES IT IN HLIM
MOV     @HALF,R1      ;R1 <-- HALF POINT OF INPUT DATA
MOV     @OFFSET,R2    ;R2 <-- OFFSET
SUB     R2,R1         ;FINDS R2-R1
MOV     R1,@NEWHLF    ;STORES RESULT IN NEWHALF
SUB     #512,R1       ;IS IT LARGER THAN THE LOWER LIMIT?
BHI     LESSL         ;IF NOT THERE WILL BE PADDING IN THE
;LEFT ARRAY
MOV     @NEWHLF,R1    ;R1 <-- NEW HALF POINT
SUB     @HLIM,R1      ;IS IT SMALLER THAN UPPER LIMIT?
BPL     LESSR         ;IF NOT THER WILL BE PADDING IN THE
;RIGHT ARRAY
;NO PADDING NECESSARY
;
OK:     MOV     @NEWHLF,R1 ;R1 <-- NEW HALF POINT
ASL     R1         ;MULTIPLY BY 2 TO GET OFFSET IN BYTES
MOV     @ARRAY,R0   ;R0 <-- STARTING ADDRESS OF INPUT ARRAY
ADD     R1,R0       ;ADD OFFSET
MOV     R0,@TEMP    ;TEMP <-- ADDRESS OF MIDDLE POINT
MOV     #512,R3     ;SET COUNTER
MOV     @RIGHT,R2   ;R2 <-- ADDRESS OF RIGHT ARRAY
LOOPR:  MOV     (R0)+,(R2)+ ;MOVE DATA TO RIGHT ARRAY
SOB     R3,LOOPR    ;REPEAT UNTILL FINISH
MOV     @TEMP,R0     ;R0 <-- ADDRESS OF MIDDLE POINT
MOV     #512,R3     ;SET COUNTER
MOV     @LEFT,R2    ;R2 <-- ADDRESS OF LEFT ARRAY
LOOPL:  MOV     -(R0),(R2)+ ;MOVE DATA TO LEFT ARRAY
SOB     R3,LOOPL    ;REPEAT UNTILL FINISH
BR      FINI        ;ALL DONE!
;
; PADDING IN LEFT ARRAY NECESSARY

```

```

;
LESSL: NEG    R1          ;
        MOV    R1, @NDIFF ;DIFF <-- # POINTS THAT WILL BE ZERO
        MOV    @NEWHLF, R1 ;R1 <-- NEW HALF POINT
        MOV    @ARRAY, R0 ;R0 <-- ADDRESS OF INPUT ARRAY
        ASL    R1          ;MULTIPLY BY 2 TO GET OFFSET IN BYTES
        ADD    R1, R0      ;ADD OFFSET
        MOV    R0, @TEMP   ;TEMP <-- ADDRESS OF MIDDLE POINT
        MOV    @NEWHLF, R3 ;R3 <-- # OF POINTS THAT WILL BE COPIED
        MOV    @LEFT, R2   ;R2 <-- ADDRESS OF LEFT ARRAY
LOOP1:  MOV    -(R0), (R2)+ ;MOVE DATA TO LEFT ARRAY
        SOB    R3, LOOP1   ;REPEAT UNTILL DONE
        MOV    @NDIFF, R3  ;R3 <-- REMAINING # OF POINTS
LOOP2:  MOV    #0, (R2)+    ;FILL WITH ZERO
        SOB    R3, LOOP2   ;REPEAT UNTILL DONE
        MOV    @TEMP, R0   ;TEMP <-- ADDRESS OF MIDDLE POINT
        MOV    #512, R3    ;SET COUNTER
        MOV    @RIGHT, R2  ;R2 <-- ADDRESS OF RIGHT ARRAY
LOOP4:  MOV    (R0)+, (R2)+ ;MOVE DATA TO RIGHT ARRAY
        SOB    R3, LOOP4   ;REPEAT UNTILL DONE
        BR     FINI        ;ALL DONE
;
;   PADDING IN RIGHT ARRAY NECESSARY
;
LESSR:  MOV    R1, @NDIFF   ;DIFF <-- # OF POINTS THAT WILL BE ZERO
        MOV    @ARRAY, R0  ;R0 <-- ADDRESS OF INPUT ARRAY
        MOV    @NEWHLF, R1 ;R1 <-- NEW HALF POINT
        ASL    R1          ;GET BYTES OFFSET
        ADD    R1, R0      ;ADD OFFSET
        MOV    R0, @TEMP   ;TEMP <-- ADDRESS OF MIDDLE POINT
        MOV    #512, R3    ;
        SUB    @NDIFF, R3  ;R3 <-- # OF POINT TO BE COPIED
        MOV    @RIGHT, R2  ;R2 <-- ADDRESS OF RIGHT ARRAY
LOOP5:  MOV    (R0)+, (R2)+ ;MOVE DATA TO RIGHT ARRAY
        SOB    R3, LOOP5   ;REPEAT UNTILL DONE
        MOV    @NDIFF, R3  ;R3 <-- # OF REMAINING POINTS
LOOP6:  MOV    #0, (R2)+    ;FILL WITH ZEROS
        SOB    R3, LOOP6   ;UNTILL DONE
        MOV    #512, R3    ;SET COUNTER
        MOV    @TEMP, R0   ;R0 <-- ADDRESS OF MIDDLE POINT
        MOV    @LEFT, R2   ;R2 <-- ADDRESS OF LEFT ARRAY
LOOP7:  MOV    -(R0), (R2)+ ;MOVE DATA TO LEFT ARRAY
        SOB    R3, LOOP7   ;REPEAT UNTILL DONE
FINI:   RTS    PC          ;RETURN
ARRAY:  0
NMAX:   0
OFFSET: 0
HALF:   0
HLIM:   0
NEWHLF: 0
RIGHT:   0
LEFT:    0
DIFF:    0
TEMP:    0
.END

```

```

CXXXXXXXXXXXXXXXXXXXXXXXXXXXXXXXXXXXXXXXXXXXXXXXXXXXXXXXXXXXXXXXXXXXXX
C
C      PROGRAM SMUTH
C
C      CALLER PROGRAM THAT  ALLOWS USER TO DO A 9-POINT SMOOTHING
C      IN ANY FILE CONTAINING REAL OR INTEGER DATA
C
CXXXXXXXXXXXXXXXXXXXXXXXXXXXXXXXXXXXXXXXXXXXXXXXXXXXXXXXXXXXXXXXXXXXXX
      REAL*8 INT,TEMP, IDNA,CAMK,CAMK2,TEMP1,SINH1,DIS2
      REAL*8 DISINC,PERIOD,LAMBOA
      DIMENSION IARR(512)
      REAL ARRAY2(512),ARRAY1(512),ARRAY4(512)
      EQUIVALENCE(IARR(1),ARRAY4(1))
      LOGICAL*1 IANS
12      FORMAT(7(E13.6))
58      FORMAT(7I7)
288     FORMAT(A6)
      N=512                !INITIALIZE
      M=2*N
      PI=3.1415926
      CALL CLEPLT          !CLEAR GRAPHICS
      TYPE X,'NAME OF FILE?' !ASK FOR NAME OF FILE
      READ(7,288) IDNA      !GET NAME OF FILE FROM KEYBOARD
      CALL ASSIGN(28,IDNA)  !OPEN THE GIVEN FILE
38      CALL CLEAR          !CLEAR SCREEN
      TYPE X,'REAL OR INTEGER?' !DOES THE FILE CONTAIN REAL OR INTEGER DATA?
      CALL INCHAR(IANS)     !GET ANSWER FROM KEYBOARD
      IF(IANS.EQ.'R') GO TO 32
      IF(IANS.NE.'I') GO TO 38
      READ(28,58)(IARR(J),J=1,N) !READ INTEGER DATA
      CALL CLEAR            !CLEAR SCREEN
      DO 1 J=1,N             !CONVERT INTEGER DATA INTO REAL
1      ARRAY1(J)=FLOAT(IARR(J))
      GO TO 17
32      READ(28,12)(ARRAY1(J),J=1,N) !READ REAL DATA
17      CALL CLOSE(28)          !CLOSE FILE
      CALL CLEPLT              !CLEAR GRAPHIC SCREEN
      CALL SMOOTH(N,ARRAY1,M,ARRAY2) !DOES THE SMOOTHING
      CALL PLTSIM(ARRAY2,ARRAY1(4),N-8,8) !PLOT THE SMOOTH & UNSMOOTH FILES
      CALL PLTSIM(ARRAY2(256),ARRAY1(268),252,8) !SHOW DETAIL OF GRAPHS
18      CALL CLEPLT            !CLEAR GRAPHICS
      TYPE X,'SATISFIED?'      !DO YOU WISH MORE SMOOTHING?
      CALL INCHAR(IANS)        !GET ANSWER
      IF(IANS.EQ.'N') GO TO 19
      IF(IANS.NE.'Y') GO TO 18
997     CALL CLEAR
      TYPE X,'DO YOU WISH TO SAVE?' !DO YOU WISH TO SAVE RESULTS?
      CALL INCHAR(IANS)          !GET ANSWER
      IF(IANS.EQ.'N') GO TO 999
      IF(IANS.NE.'Y') GO TO 997
      CALL CLEAR
      TYPE X,'UNDER WHAT NAME?'    !ASK FOR THE NAME OF FILE TO BE CREATED
      READ(7,288) IDNA             !GET THE NAME
      DO 3 J=1,4                   !SET UP THE DATA INTO PROPER FORM
      ARRAY1(J)=ARRAY2(1)
3      ARRAY1(N-J+1)=ARRAY2(504)
      DO 4 J=1,N-8
4      ARRAY1(J+4)=ARRAY2(J)

```

```

      CALL ASSIGN(20, IDNA)
      WRITE(20, 12) (ARRAY1(J), J=1, N) !WRITE THE FILE
      CALL CLOSE(20)
      GO TO 999
19    DO 2 J=1, N-8      !REINITIALIZE ARRAYS FOR NEXT SMOOTHING
2    ARRAY1(J+4)=ARRAY2(J)
      GO TO 17
999   CALL CLEPLT      !ALL DONE
      CALL EXIT
      END
CXXXXXXXXXXXXXXXXXXXXXXXXXXXXXXXXXXXXXXXXXXXXXXXXXXXXXXXXXXXXXXXXXXXXX
C
C   SUBROUTINE TO DO 9-POINT SMOOTHING USING LEAST SQUARES
C   TECHNIQUES.
C
C   CALLER PROGRAM: SMUTH
C
C   FOR DETAILS SEE REFERENCE 27
C
C   DATA LINKAGE:
C     INPUT-
C       N      NUMBER OF RAW DATA POINTS
C       DATAIN ARRAY CONTAINING N DATA POINTS
C     OUTPUT-
C       M      NUMBER OF SMOOTH DATA POINTS
C       DATAO  ARRAY CONTAINING SMOOTHED DATA POINTS
C
CXXXXXXXXXXXXXXXXXXXXXXXXXXXXXXXXXXXXXXXXXXXXXXXXXXXXXXXXXXXXXXXXXXXXX
      SUBROUTINE SMOOTH(N, DATAIN, M, DATAO)
      REAL DATAIN(N), DATAO(N), NP(9)
      M=N-8
      DO 10 I=2, 9
        J=I-1
10     NP(I)=DATAIN(J)
        DO 200 I=1, M
          J=I+8
          DO 11 K=1, 8
            KA=K+1
11     NP(K)=NP(KA)
            NP(9)=DATAIN(J)
            SUM=52.*NP(5)+54.*X(NP(4)+NP(6))+39.*X(NP(3)+NP(7))+14.*X(NP(2)+
            NP(8))-21.*X(NP(1)+NP(9))
            DATAO(I)=SUM/231.
200    CONTINUE
      RETURN
      END

```



```

CXXXXXXXXXXXXXXXXXXXXXXXXXXXXXXXXXXXXXXXXXXXXXXXXXXXXXXXXXXXXXXXXXXXXX
C
C      PROGRAM NORM
C
CXXXXXXXXXXXXXXXXXXXXXXXXXXXXXXXXXXXXXXXXXXXXXXXXXXXXXXXXXXXXXXXXXXXXX
C
C      THIS PROGRAM DOES THE FOLLOWING:
C      1) CONVERTS DATA FROM TRANSMISSION VALUES TO DIFFUSE DENSITY VALUES
C      2) FINDS NORMALIZATION CONSTANT
C
C      FOR DETAILS SEE CHAPTER IV
C
C      REAL*8 INT,TEMP, IDNA,CAMK,CAMK2,TEMP1,SINHT,DIS2
C      REAL*8 DISINC,PERIOD,LAMBOA
C      DIMENSION IARR(512)
C      REAL ARRAY2(512),ARRAY1(512),ARRAY4(512)
C      EQUIVALENCE(IARR(1),ARRAY4(1))
C      LOGICAL*1 IANS
C      INTEGER TMAX
12      FORMAT(7(E13.6))
58      FORMAT(7I7)
200     FORMAT(A6)
C      N=512
C      M=2*N
C      PI=3.1415926
C      CALL CLEPLT           !INITIALIZE GRAPHICS
C      TYPE X,'NAME OF FILE?' !ASK FOR THE DATA FILE TO BE PROCESSED
C      READ(7,200) IDNA       !GET ANSWER FROM KEYBOARD
C      CALL ASSIGN(20,IDNA)    !OPEN THE FILE
C      READ(20,12)(ARRAY1(J),J=1,N) !READ THE DATA
C      CALL CLOSE(20)         !CLOSE THE FILE
C      CALL CLEAR             !CLEAR SCREEN
C      TYPE X,'NAME OF FILE CONTAINING T-MAX?' !ASK FOR FILE WITH T-MAX
C      READ(7,200) IDNA       !GET ANSWER FROM KEYBOARD
C      CALL ASSIGN(20,IDNA)    !OPEN FILE
C      READ(20,58) TMAX       !READ DATA
C      CALL CLOSE(20)         !CLOSE FILE
C      CALL CLEAR             !CLEAR SCREEN
C      DO 1 I=1,N             !INITIALIZE ARRAY2 TO T-MAX
1      ARRAY2(I)=TMAX
C      TYPE X,'NAME OF FILE CONTAINING A.S.F.?' !ASK FOR FILE WITH ATOMIC
C      !SCATTERING FACTORS SQUARED
C      READ(7,200) IDNA       !GET ANSWER
C      CALL ASSIGN(20,IDNA)    !OPEN FILE
C      READ(20,12)(ARRAY4(J),J=1,N) !READ DATA
C      CALL CLOSE(20)         !CLOSE FILE
C      CALL PLTSIM(ARRAY1,ARRAY2,N,0) !PLOT DATA & T-MAX
C      CALL CLEPLT           !CLEAR GRAPHICS
C      DO 10 I=1,N            !INITIALIZE ARRAY2 TO ZERO
C      ARRAY2(I)=0.
10     ARRAY1(I)=ALOG10(TMAX/ARRAY1(I)) !CALCULATE DIFFUSE DENSITY
C      CALL PLTSIM(ARRAY1,ARRAY2,N,0) !PLOT DIFFUSE DENSITY
17     CALL CLEPLT           !CLEAR GRAPHICS
C      TYPE X,'CONSTANT'      !ASK FOR NORMALIZATION CONSTANT
C      ACCEPT X,CONST         !GET CONSTANT
C      DO 16 I=1,N            !NORMALIZE DATA
16     ARRAY2(I)=CONST*ARRAY1(I)
C      CALL PLTSIM(ARRAY4(256),ARRAY2(256),256) !PLOT DATA & A.S.F.

```

Appendix 2

```

18  CALL CLEPLT          !CLEAR GRAPHICS
    TYPE X,'SATISFIED?'  !GOOD ENOUGH?
    CALL INCHAR(IANS)    !GET ANSWER
    IF(IANS.EQ.'N') GO TO 17 !IF NOT GO BACK FOR ANOTHER CONSTANT
    IF(IANS.NE.'Y') GO TO 18
997  CALL CLEPLT          !CLEAR GRAPHICS
    TYPEX,'DO YOU WISH TO SAVE?' !SAVE DATA?
    CALL INCHAR(IANS)    !GET ANSWER
    IF(IANS.EQ.'N') GO TO 999 !IF NOT GO TO FINISH
    IF(IANS.NE.'Y') GO TO 997
    CALL CLEAR           !CLEAR SCREEN
    TYPEX,'UNDER WHAT NAME?' !ASK FOR NAME OF FILE TO BE WRITTEN INTO
    READ(7,200) IDNA     !GET NAME
    CALL ASSIGN(20,IDNA) !OPEN FILE
    WRITE(20,12) CONST    !WRITE NORMALIZATION COSTANT
    WRITE(20,12)(ARRAY1(J),J=1,N) !WRITE DATA
    CALL CLOSE(20)        !CLOSE FILE
999  CALL CLEPLT          !CLEAR GRAPHICS
    CALL EXIT            !STOP
    END

```

```

XXXXXXXXXXXXXXXXXXXXXXXXXXXXXXXXXXXXXXXXXXXXXXXXXXXXXXXXXXXX
C
C   PROGRAM ISPLOT
C
CXXXXXXXXXXXXXXXXXXXXXXXXXXXXXXXXXXXXXXXXXXXXXXXXXXXXXXXXXXXX
C
C   THIS PROGRAM GIVES A CHART RECORDER OUTPUT FOR THE FUNCTION
C   i(s). FROM THIS GRAPH THE ERROR FUNCTION EPSILON CAN BE
C   DETERMINED
C   FOR DETAILS SEE CHAPTER IV SECTION iv
C
C   REAL ATOFAC(512),ARRAY(1024),HALF(512)
C   REALX8 IDNA,CAMK,RSTEP,ACCPOT
C   REALX8 CAMK2,LAMBDA,PI,DISINC,DIS2,SHAX,RRES,RMAX
C   LOGICALX1 IANS
C   COMMON/BLOCK/LAMBDA,CAMK,SINC
C   PI=3.1415926
12  FORMAT(7(E13.6))
58  FORMAT(7I7)
288 FORMAT(A6)
281 FORMAT(' S-MAX=',F7.4,' S-STEP=',F7.4,' R RESOLUTION=',F7.4,
8' R-MAX IN GRAPH=',F10.4,' R STEP=',F13.10)
282 FORMAT(11F6.1)
283 FORMAT(I7)
C   CALL CLEPLT
C+++++
C
C   NICKEL DATA
C
C-----
C   CAMK=250.0      !CAMERA CONSTANT
C   DISINC=0.8367   !DISTANCE THAT DENSITOMETER MOVED FOR
C                   !EACH POINT ACQUIRED
C   ACCPOT=100.0E03 !ACCELERATING POTENTIAL
C+++++
C   CALL MAXLEN(ACCPOT,LAMBDA) !FIND THE WAVELENGTH OF THE ELEC. BEAM
C   N=512           !NUMBER OF POINTS IN DATA FILE
C   M=2XN
C   SHAX=SVAL(N)    !MAXIMUM VALUE OF S IN DATA FILE
C   RRES=1.0/(2.0XSHAX) !RESOLUTION IN R SPACE
C   RMAX=1.0/(2.0XSVAL(2)) !MAXIMUM VALUE OF R
C   RSTEP=RMAX/FLOAT(N-1) !R INCREMENT
C   DO 33 J=1,M     !INITIALIZE
33  ARRAY(J)=0.0
C   TYPE X,'EXECUTING ISPLOT PROGRAM'
C   WRITE(5,201)SHAX,SVAL(2),RRES,RMAX/4,RSTEP
C   TYPE X,'NAME OF DATA FILE?' !ASK FOR NAME OF DATA FILE
C   READ(7,200) IDNA !GET NAME
C   CALL ASSIGN(20,IDNA) !OPEN FILE
C   READ(20,12)CONST !READ NORMALIZATION CONSTANT
C   READ(20,12)(HALF(J),J=1,N) !READ DATA
C   CALL CLOSE(20) !CLOSE FILE
C   CALL PLTSIM(HALF,ARRAY,N,8) !PLOT DATA
C   CALL CLEAR !CLEAR SCREEN
C   TYPE X,'NAME OF FILE CONTAINING A.S.F.' !ASK FOR NAME OF FILE WITH
C                   !ATOMIC SCATTERING FACTORS SQUARED
C   TYPE X,'NAME OF FILE CONTAINING A.S.F.'
C   READ(7,200) IDNA !GET NAME

```

```

CALL ASSIGN(20, IDNA) !OPEN THE FILE
READ(20, 12) (ATOFAC(J), J=1, N) !READ THE A.S.F
CALL CLOSE(20) !CLOSE THE FILE
CALL CLEAR !CLEAR SCREEN
DO 21 J=1, N !CALCULATE i(s)
S=SVAL(J)
21 HALF(J)=SX(((HALF(J)*CONST/ATOFAC(J))-1)
CALL PLTSIM(HALF, ARRAY, N, 0) !PLOT IN SCREEN i(s)
22 CALL CLEAR !CLEAR SCREEN
TYPE X, 'READY?' !READY TO USE CHART RECORDER
CALL INCHAR(IANS) !GET ANSWER
IF(IANS.NE.'Y') GO TO 22 !IF NOT ASK AGAIN
CALL CLEAR !CLEAR SCREEN
CALL QUANT(HALF, ARRAY, M, N) !DOES QUADRATIC INTERPOLATION IN DATA
C !SO THAT THE NUMBER OF POINTS PLOTTED IN THE
C !CHART RECORDER IS DOUBLED
CALL PLOTDA(ARRAY, M, 1) !PLOT IN CHART RECORDER VIA D/A
CALL BELL !RING BELL WHEN DONE PLOTTING
999 CALL CLEPLT !CLEAR GRAPHICS
CALL EXIT !STOP
END

```

```

CXXXXXXXXXXXXXXXXXXXXXXXXXXXXXXXXXXXXXXXXXXXXXXXXXXXXXXXXXXXX
C
C      PROGRAM CHA
C
C      THIS PROGRAM CORRECTS i(s) FROM THE ADDITIVE ERROR
C      FUNCTION EPSALON
C      FOR DETAILS SEE CHAPTER IV SECTION iv
C
CXXXXXXXXXXXXXXXXXXXXXXXXXXXXXXXXXXXXXXXXXXXXXXXXXXXXXXXXXXXX
C      REAL ATOFAC(512),ARRAY(1024),N1(1024),X1(70),DATUM(70)
C      DIMENSION HALF(512),GAUSS(512)
C      EQUIVALENCE(ATOFAC(1),GAUSS(1))
C      REALX8 IDNA,CAMK,RSTEP,ACCPOT
C      REALX8 CAMK2,LAMBDA,PI,DISINC,DIS2,SMAX,RRES,RMAX
C      LOGICALX1 TANS
C      COMMON/BLOCK/LAMBDA,CAMK,DISINC
C      PI=3.1415926
12      FORMAT(7(E13.6))
58      FORMAT(7I7)
200     FORMAT(A6)
201     FORMAT(' S-MAX=',F7.3,' S-STEP=',F7.3,' R RESOLUTION=',F7.3,
8' R-MAX IN GRAPH=',F7.3,' R STEP=',F7.3)
202     FORMAT(11F7.2)
203     FORMAT(17)
C      RMIN=1.0E6
C      HMAX=-1.0E6
C      PI=3.1415926
C      CALL CLEPLT/              !INITIALIZE GRAPHICS
C+++++
C
C      NICKEL
C-----
C      CAMK=250.8                !CAMERA CONSTANT
C      DISINC=0.03667            !DISTANCE THAT DENSITOMETER MOVED FOR
C                                !EACH POINT ACQUIRED
C      ACCPOT=100.0E03           !ACCELERATING POTENTIAL
C+++++
C      CALL WAVLEN(ACCPOT,LAMBDA) !FIND THE WAVELENGTH OF THE ELEC. BEAM
C      N=512                      !NUMBER OF POINTS IN DATA FILE
C      M=2*N
C      SMAX=SVAL(N)               !MAXIMUM VALUE OF S IN DATA FILE
C      RRES=1.0/(2.0*SMAX)        !RESOLUTION IN R SPACE
C      RMAX=1.0/(2.0*SVAL(2))     !MAXIMUM VALUE OF R
C      RSTEP=RMAX/FLOAT(N-1)     !R INCREMENT
C      DO 33 J=1,M               !INITIALIZE
33      ARRAY(J)=0.0
C      TYPE X,'EXECUTING PROGRAM CHA'
C      WRITE(5,201)SMAX,SVAL(2),RRES,RMAX/4,RSTEP
C      TYPE X,'NAME OF DATA FILE?' !ASK FOR NAME OF DATA FILE
C      READ(7,200) IDNA           !GET NAME
C      CALL ASSIGN(20,IDNA)       !OPEN FILE
C      READ(20,12)CONST           !READ NORMALIZATION COSTANT
C      READ(20,12)(HALF(J),J=1,N) !READ DATA
C      CALL CLOSE(20)             !CLOSE FILE
C      CALL CLEAR                 !CLEAR SCREEN
C      TYPE X,'NAME OF FILE CONTAINING A.S.F.' !ASF FOR NAME OF FILE WITH
C                                !ATOMIC SCATTERING FATORS SQUARED

```

```

      READ(7,280) IDNA      !GET NAME
      CALL ASSIGN(28,IDNA)  !OPEN FILE
      READ(28,12) (ATOFAC(J),J=1,N) !READ A.S.F.
      CALL CLOSE(28)       !CLOSE FILE
      CALL CLEAR           !CLEAR SCREEN
      DO 21 J=1,N          !CALCULATE i(s)
      S=SVAL(J)
21  HALF(J)=SX((HALF(J)*CONST/ATOFAC(J))-1)
      DO 51 J=1,N          !FIND MAX. & MIN VALUES OF i(s)
      IF(HALF(J).GT.HMAX) GO TO 52
53  IF(HALF(J).LT.RMIN) GO TO 54
51  CONTINUE
      GO TO 55
52  HMAX=HALF(J)
      GO TO 53
54  RMIN=HALF(J)
      GO TO 51
55  CALL PLTSIM(HALF,ARRAY,N,0) !PLOT i(s)
      CALL CLEPLT          !CLEAR GRAPHICS
C
C  THE ERROR FUNCTION IS ENTER AS SERIES OF EQUALLY SPACED
C  POINTS OF ARBITRARY UNITS
C
      TYPE X,'NAME IF INPUT FILE?' !ASK FOR NAME OF FILE WITH
C
      READ(7,280) IDNA      !ERROR FUNCTION POINTS
      CALL ASSIGN(28,IDNA)  !GET NAME
      READ(28,283) NN       !OPEN FILE
      READ(28,282) CHMAX    !READ # OF POINTS IN ERROR FUNCTION
      READ(28,282) CHMAX    !READ MAXIMUM VALUE
      READ(28,282) (DATUM(J),J=1,NN) !READ ERROR FUNCTION POINTS
      CALL CLOSE(28)       !CLOSE FILE
      STEP=SVAL/FLOAT(NN-1) !X-AXIS INCREMENT
      STEP2=HMAX/CHMAX      !Y-AXIS NORMALIZATION
      DO 2 J=1,NN
      X1(J)=(J-1)*STEP      !NORMALIZE X-AXIS
2  DATUM(J)=DATUM(J)*STEP2 !NORMALIZE Y-AXIS
      DO 61 J=1,N           !INTERPOLATE ERROR CURVESO THAT IT
      S=SVAL(J)             !COVERS ALL 512 POINTS, UP TO S-MAX
      CALL CURGEN(DATUM,X1,S,Y,NN) !INTERPOLATION ROUTINE
      ARRAY(J)=Y            !STORES ERROR FUNCTION VALUES IN ARRAY
61  CONTINUE
      CALL PLTSIM(HALF,ARRAY,N,0) !PLOT i(s) & ERROR FUNCTION
      CALL CLEPLT          !CLEAR GRAPHICS
      DO 62 J=1,N
      HALF(J)=HALF(J)-ARRAY(J) !SUBTRACT ERROR FUNCTION
62  ARRAY(J)=0.
      CALL PLTSIM(HALF,ARRAY,N,0) !PLOT CORRECTED i(s)
76  CALL CLEPLT          !CLEAR GRAPHICS
      TYPE X,'DO YOU WISH TO SAVE?' !SAVE RESULTS?
      CALL INCHAR(IANS)      !GET ANSWER
      IF(IANS.EQ.'N') GO TO 999 !IF NOT, GO TO FINISH
      IF(IANS.NE.'Y') GO TO 76
      CALL CLEAR           !CLEAR SCREEN
      TYPE X,'UNDER WHAT NAME?' !ASK FOR NAME OF FILE TO BE CREATED
      READ(7,280) IDNA      !GET NAME
      CALL ASSIGN(28,IDNA)  !OPEN FILE
      WRITE(28,12) (HALF(J),J=1,N) !WRITE RESULTS
      CALL CLOSE(28)       !CLOSE FILE
999  CALL CLEAR          !CLEAR SCREEN

```

```

CALL EXIT      !STOP
END
CXXXXXXXXXXXXXXXXXXXXXXXXXXXXXXXXXXXXXXXXXXXXXXXXXXXXXXXXXXXXXXXXXXXX
C  THIS ROUTINE INTERPOLATES THE VALUE OF A FUNCTION AT ANY VALUE
C  OF THE X-AXIS.
C  THE FUNCTION MUST BE INPUTED AS A SERIES OF VALUES FOR SPECIFIC
C  VALUES OF X
C  THE PROGRAM USES QUADRATIC INTERPOLATION TO FIND A NEW VALUE OF
C  THE FUNCTION BEING CONSIDERED
C
C  FOR DETAILS OF THE QUADRATIC INTERPOLATION TECHNIQUE USED SEE:
C  E. KREYSZIG, ADVANCED ENGINEERING MATHEMATICS,
C  CHAPTER 19, PAGE 774
C
C  CALLER PROGRAM: CHA
C
C  DATA LINKAGE:
C      INPUT-
C          ARRAY1  VALUE OF FUNCTION AT POINTS DEFINED BY X1
C          X1      VALUES OF X FOR WHICH THE FUNCTION HAS A
C                  DEFINED VALUE
C          M       NUMBER OF POINTS IN ARRAY1 & X1
C          XX      VALUE OF X FOR WHICH THE VALUE OF THE
C                  FUNCTION IS BEING SEEK
C      OUTPUT-
C          FX      INTERPOLATED VALUE OF THE FUNCTION AT
C                  POINT XX
C
CXXXXXXXXXXXXXXXXXXXXXXXXXXXXXXXXXXXXXXXXXXXXXXXXXXXXXXXXXXXXXXXXXXXX
C  SUBROUTINE CURGEN(ARRAY1,X1,XX,FX,M)
C  DIMENSION ARRAY1(M),X1(M)
C  CALL BINSER(XX,X1,M,I) !USE A BINARY SEARCH TECHNIQUE TO FIND
C                          !THE INTERVAL IN WHICH THE NEW POINT FALLS
C
C  IF(1.GE.M-1) I=M-2
C  XX0=X1(I)
C  XX1=X1(I+1)
C  XX2=X1(I+2)
C  H=(XX2-XX0)/2
C  FX0=ARRAY1(I)
C  FX1=ARRAY1(I+1)
C  FX2=ARRAY1(I+2)
C  DF0=FX1-FX0
C  DF1=FX2-FX1
C  D2F0=DF1-DF0
C  R=(XX-XX0)/H
C  FX=FX0+(R*DF0)+(R*(R-1)*.5*D2F0)
C  RETURN
C  END
C
CXXXXXXXXXXXXXXXXXXXXXXXXXXXXXXXXXXXXXXXXXXXXXXXXXXXXXXXXXXXXXXXXXXXX
C  ROUTINE TO FIND THE INTERVAL IN WHICH ANY NUMBER FALLS IN A
C  LIST OF GIVEN NUMBERS
C
C  FOR REFERENCES SEE:
C  D.E. KNUTH, "THE ART OF COMPUTER PROGRAMING VOL.3, SORTING
C  AND SEARCHING", PAGES 486/488, ADDISON WESLEY: READING MASS. 1973
C
C  CALLER PROGRAM: CURGEN
C

```

Appendix 2

```

C      DATA LINKAGE:
C      INPUT-
C          XX  ARRAY CONTAINING NUMBER LIST
C          X1  SEARCH VALUE
C          M   NUMBER OF VALUES IN LIST
C      OUTPUT-
C          I   LOCATION OF NUMBER IN LIST THAT IMMEDIATELY
C              PRECEEDS THE SEARCH VALUE
C
CXXXXXXXXXXXXXXXXXXXXXXXXXXXXXXXXXXXXXXXXXXXXXXXXXXXXXXXXXXXXXXXXXXXX
C      SUBROUTINE BINSER(XX,X1,M,I)
C      DIMENSION X1(M)
C      INTEGER FIRST,FLAG
C      FLAG=0
C      FIRST=1
C      LAST=M
C      1  IF(FLAG.EQ.1) GO TO 38
C          IF(LAST.EQ.FIRST+1) FLAG=1
C          MIDDLE=(FIRST+LAST)/2
C          IF(X1(MIDDLE).LT.X1) GO TO 18
C          IF(X1(MIDDLE).GT.X1) GO TO 20
C      38  I=MIDDLE
C          RETURN
C      18  FIRST=MIDDLE
C          GO TO 1
C      20  LAST=MIDDLE
C          GO TO 1
C      END

```



```

CXXXXXXXXXXXXXXXXXXXXXXXXXXXXXXXXXXXXXXXXXXXXXXXXXXXXX
C
C   PROGRAM KAP
C
C   THIS PROGRAM CORRECTS FOR SYSTEMATIC ERRORS CAUSED BY
C   ERRONEOUS NORMALIZATION AND INCORRECT ATOMIC SCATTERING
C   FACTORS.
C
C   FOR DETAILS SEE CHAPTER IV SECTION ii
C
CXXXXXXXXXXXXXXXXXXXXXXXXXXXXXXXXXXXXXXXXXXXXXXXXXXXXX
REAL ARRAY(512),N1(1024)
DIMENSION HALF(512),GAUSS(512)
EQUIVALENCE(N1(513),HALF)
REAL*8 IDNA,CAMK,RSTEP,ACCPOT
REAL*8 CAMK2,LAMBDA,PI,DISINC,DIS2,SHAX,RRES,RMAX
LOGICAL*1 IANS
COMMON/BLOCK/LAMBDA,CAMK,DISINC
PI=3.1415926
12  FORMAT(7(E13.6))
58  FORMAT(7I7)
200  FORMAT(A6)
201  FORMAT(' S-MAX=',F7.3,' S-STEP=',F7.3,' R RESOLUTION=',F7.3,
8' R-MAX IN GRAPH=',F7.3,' R STEP=',F7.3)
CALL CLEPLT
C+++++
C
C   NICKEL
C
C-----
CAMK=250.0
DISINC=0.03667
ACCPOT=100.0E3
C+++++
N=512          !NUMBER OF POINTS IN DATA FILE
M=2*N
CALL WAVELEN(ACCPOT,LAMBDA) !FIND WAVELENGTH OF ELECTRON BEAM
SHAX=SVAL(N)    !MAXIMUM VALUE OF S IN DATA FILE
RRES=1.0/(2.*SHAX) !RESOLUTION IN R SPACE
RMAX=1.0/(2.*SVAL(2)) !MAXIMUM VALUE OF R
RSTEP=RMAX/FLOAT(N-1) !R INCREMENT FOR EACH POINT
DO 33 J=1,N      !INITIALIZE
33  ARRAY(J)=0.0
TYPE X,'EXECUTING KAP CORRECTION PROCEDURE'
WRITE(5,201)SHAX,SVAL(2),RRES,RMAX/4,RSTEP
TYPE X,'NAME OF DATA FILE?' !ASK FOR NAME OF DATA FILE
READ(7,200) IDNA !GET NAME
CALL ASSIGN(20,IDNA) !OPEN FILE
READ(20,12)(HALF(J),J=1,N) !READ DATA
CALL CLOSE(20) !CLOSE FILE
CALL PLTSIM(HALF,ARRAY,N,0) !PLOT INPUT DATA
75  DO 50 J=1,N !STORE INPUT DATA IN ARRAY
50  ARRAY(J)=HALF(J)
CALL CLEPLT !CLEAR GRAPHICS
DO 49 I=1,N !CREATE ODD FUNCTION
49  N1(I)=HALF(513-I)
CALL FORRT(N1,N) !DO FOURIER TRANSFORM
CALL PLOT(HALF,N) !PLOT REDUCED R.D.F.

```

```

34  CALL CLEPLT          !CLEAR GRAPHICS
    TYPE X,'CUT-OFF?'   !ASK FOR END POINT OF ONDULATIONS
C    !BEFORE FIRST PEAK
    ACCEPT X,L2         !GET POINT
    CALL PLOT(HALF,L2)   !PLOT PROBLEM REGION
32  CALL CLEPLT          !CLEAR GRAPHICS
    TYPE X,'SATISFIED?' !GOT ALL POINTS?
    CALL INCHAR(IANS)    !GET ANSWER
    IF(IANS.EQ.'N') GO TO 34 !IF NOT, REPEAT
    IF(IANS.NE.'Y') GO TO 32
    DO 48 J=1,L2         !SAVE POINTS IN SELECTED REGION
48  GAUSS(J)=HALF(J)
116 CALL CLEAR          !CLEAR SCREEN
    TYPE X,'SLOPE?'     !ASK FOR SLOPE OF LINE
    ACCEPT X,SLOPE      !GET THE SLOPE
    DO 38 J=1,L2        !CREATE LINE OF SPECIFIED SLOPE IN THE
38  HALF(J)=-SLOPEX(FLOAT(J-1)*XRSTEP) !SELECTED REGION
    CALL PLOT(HALF,N)    !PLOT NEW REDUCED RDF
117 CALL CLEPLT          !CLEAR GRAPHICS
    TYPE X,'SATISFIED?' !IS THE SLOPE GOOD ENOUGH?
    CALL INCHAR(IANS)    !GET ANSWER
    IF(IANS.EQ.'N') GO TO 116 !IF NOT, CHOOSE A DIFFERENT SLOPE
    IF(IANS.NE.'Y') GO TO 117
    DO 31 J=1,L2        !CALCULATE THE DIFFERENCE FUNCTION
31  HALF(J)=HALF(J)-GAUSS(J)
    DO 73 J=L2+1,N-1
73  HALF(J)=0.0
    CALL PLOT(HALF,N)    !PLOT DIFFERENCE FUNCTION
    CALL CLEPLT          !CLEAR GRAPHICS
    DO 81 J=1,N-1
81  N1(J)=0.0           !SET FIRST HALF OF INPUT ARRAY OF THE
    CALL REVRT(N1,N)     !INVERSE FOURIER TRANSFORM TO ZERO
    CALL PLOT(HALF,N)    !DO THE INVERSE TRANSFORM
    CALL PLOT(HALF,N)    !PLOT ERROR TRANSFORM FUNCTION
    CALL CLEPLT          !CLEAR GRAPHICS
    DO 72 J=2,N-1        !CALCULATE THE NEW i(s)
72  S=SVAL(J)
    HALF(J)=(HALF(J)*(ARRAY(J)/S))+ARRAY(J)+HALF(J)
    HALF(1)=0            !FIX THE FIRST AND LAST POINT
    HALF(N)=HALF(N-1)
    CALL PLOT(HALF,N)    !PLOT THE CORRECTED i(s)
74  CALL CLEPLT          !CLEAR GRAPHICS
    TYPE X,'SATISFIED?' !GOOD ENOUGH?
    CALL INCHAR(IANS)    !GET ANSWER
    IF(IANS.EQ.'N') GO TO 75 !IF NOT WE CAN DO THE WHOLE PROCESS ALL
C    !OVER AGAIN
    IF(IANS.NE.'Y') GO TO 74
76  CALL CLEAR
    TYPE X,'DO YOU WISH TO SAVE?' !SAVE RESULTS?
    CALL INCHAR(IANS)    !GET ANSWER
    IF(IANS.EQ.'N') GO TO 999 !IF NOT, GO TO END
    IF(IANS.NE.'Y') GO TO 76
    CALL CLEAR          !CLEAR SCREEN
    TYPE X,'UNDER WHAT NAME?' !ASK THE NAME OF THE FILE TO BE CREATED
    READ(7,200) IDNA     !GET NAME
    CALL ASSIGN(20,IDNA) !OPEN FILE
    WRITE(20,12) (HALF(J),J=1,N) !WRITE DATA
    CALL CLOSE(20)       !CLOSE FILE
999 CALL CLEAR          !CLEAR SCREEN
    CALL EXIT            !STOP

```

```

CXXXXXXXXXXXXXXXXXXXXXXXXXXXXXXXXXXXXXXXXXXXXXXXXXXXXXXXXXXXX
C
C      PROGRAM RDF
C
C      PROGRAM TO GENERATE REDUCED RADIAL DISTRIBUTION FUNCTIONS
C      USES THE HANNING FUNCTION AS THE TERMINATION FUNCTION
C
CXXXXXXXXXXXXXXXXXXXXXXXXXXXXXXXXXXXXXXXXXXXXXXXXXXXXXXXXXXXX
C      REAL ARRAY(512),N1(1024)
C      DIMENSION HALF(512),GAUSS(512)
C      EQUIVALENCE(N1(513),HALF)
C      REAL*8 IDNA,CAMK,RSTEP,ACCPOT
C      REAL*8 CAMK2,LAMBDA,PI,DISINC,DIS2,SMAX,RRES,RMAX
C      LOGICAL*1 IANS
C      COMMON/BLOCK/LAMBDA,CAMK,DISINC
C      PI=3.1415926
12  FORMAT(7(E13.6))
58  FORMAT(7I7)
200  FORMAT(A6)
201  FORMAT(' S-MAX=',F7.3,/' S-STEP=',F7.3,/' R RESOLUTION=',F7.3,/'
      R-MAX IN GRAPH=',F7.3,/' R STEP=',F7.3)
C      CALL CLEPLT
C+++++
C
C      NICKEL
C
C-----
C      CAMK=250.0
C      DISINC=0.03667
C      ACCPOT=100.0E3
C+++++
C      N=512          !NUMBER OF POINTS IN DATA FILE
C      M=2*N
C      CALL WAVLEN(ACCPOT,LAMBDA) !FIND WAVELENGTH OF ELECTRON BEAM
C      SMAX=SVAL(N)      !MAXIMUM VALUE OF S IN DATA FILE
C      RRES=1.0/(2.*SMAX) !RESOLUTION IN R SPACE
C      RMAX=1.0/(2.*SVAL(2)) !MAXIMUM VALUE OF R
C      RSTEP=RMAX/FLOAT(N-1) !R INCREMENT FOR EACH POINT
C      DO 33 J=1,N      !INITIALIZE
33  ARRAY(J)=0.0
C      TYPE X,'CALCULATING RDF FOR NICKEL'
C      WRITE(5,201) SMAX,SVAL(2),RRES,RMAX/4,RSTEP
C      TYPE X,'NAME OF DATA FILE?' !ASK FOR NAME OF DATA FILE
C      READ(7,200) IDNA      !GET NAME
C      CALL ASSIGN(20,IDNA)  !OPEN FILE
C      READ(20,12)(HALF(J),J=1,N) !READ DATA, THE i(s) FUNCTION
C      CALL CLOSE(20)        !CLOSE THE FILE
C      CALL PLTSIM(HALF,ARRAY,N,0) !PLOT THE DATA
C      CALL CLEPLT          !CLEAR GRAPHICS
C      DO 30 I=1,N          !CREATE AN ODD FUNCTION
30  N1(I)=-HALF(N+1-I)
C      DO 28 J=1,M          !MULTIPLY BY TERMINATING FUNCTION
28  N1(J)=N1(J)*0.5+0.5*COS(PI*FLOAT(J-1)/FLOAT(N))
C      CALL FORRT(N1,M)      !PERFORM TRANSFORM
C      CALL PLOT(HALF,N)     !PLOT REDUCED RDF
92  CALL CLEPLT            !CLEAR GRAPHICS
C      DO 26 J=1,N          !NORMALIZE
26  HALF(J)=8.*PI*HALF(J)

```

```

      CALL QUANT(HALF,GAUSS,N,N/4) !EXPAND SECTION OF INTEREST TO
C      !512 POINTS
      CALL PLOT(GAUSS,N) !PLOT RESULTS
      CALL CLEPLT !CLEAR GRAPHICS
      TYPEX,'DO YOU WISH TO SAVE?' !SAVE RESULTS?
      CALL INCHAR(IANS) !GET ANSWER
      IF(IANS.EQ.'N') GO TO 899 !IF NOT GO TO END
      IF(IANS.NE.'Y') GO TO 92
      CALL CLEAR !CLEAR SCREEN
      TYPE X,'UNDER WHAT NAME?' !ASK NAME OF FILE TO BE CREATED
      READ(7,200) IDNA !GET NAME
      CALL ASSIGN(20,IDNA) !OPEN FILE
      WRITE(20,12)(GAUSS(J),J=1,N) !WRITE REDUCED RDF
      CALL CLOSE(20) !CLOSE FILE
899  CALL CLEPLT !CLEAR GRAPHICS
      CALL EXIT !STOP
      END
CXXXXXXXXXXXXXXXXXXXXXXXXXXXXXXXXXXXXXXXXXXXXXXXXXXXXXXXXXXXXXXXXXXXXX
C
C      PROGRAM QUANT
C
C      SUBROUTINE TO DO QUADRATIC INTERPOLATION
C
C      CALLER PROGRAMS: ISPLT,RDF
C
C
C      LINKAGE:
C      ARRAY1 - ARRAY CONTAINING ORIGINAL DATA
C      ARRAY2 - WILL CONTAIN INTERPOLATED DATA
C      N - DIMENSION OF ARRAY2, N=NUMXM
C      M - DIMENSION OF ARRAY1
C
C      FOR REFERENCES SEE - E. KREYSZIG,ADVANCED ENGINEERING MATHEMATICS,
C      CHAPTER 19,PAGE 774
C
CXXXXXXXXXXXXXXXXXXXXXXXXXXXXXXXXXXXXXXXXXXXXXXXXXXXXXXXXXXXXXXXXXXXXX
      SUBROUTINE QUANT(ARRAY1,ARRAY2,N,M)
      DIMENSION ARRAY1(M),ARRAY2(N)
      NUM=N/M
      J=0
      DO 10 I=1,M-2
        X0=I-1
        X1=I
        X2=I+1
        H=(X2-X0)/2
        FX0=ARRAY1(I)
        FX1=ARRAY1(I+1)
        FX2=ARRAY1(I+2)
        J=J+1
        ARRAY2(J)=FX0
        DF0=FX1-FX0
        DF1=FX2-FX1
        D2F0=DF1-DF0
        DO 20 JJ=1,NUM-1
          X=X0+FLOAT(JJ)/FLOAT(NUM)
          R=(X-X0)/H
          FX=FX0+(RXDF0)+(RX(R-1)*.5XD2F0)
          J=J+1
          ARRAY2(J)=FX

```

```

18  CONTINUE
    DO 38 I=1,2
      J=J+1
      ARRAY2(J)=ARRAY1(N-2+I)
      DO 48 JJ=1,NUM-1
        IF(I.EQ.1)X=X1+FLOAT(JJ)/FLOAT(NUM)
        IF(I.EQ.2)X=X2+FLOAT(JJ)/FLOAT(NUM)
        R=(X-X0)/H
        FX=FX0+(RXDF0)+(RX(R-1))*5XD2F0
        J=J+1
48    ARRAY2(J)=FX
38  CONTINUE
    RETURN
    END
CXXXXXXXXXXXXXXXXXXXXXXXXXXXXXXXXXXXXXXXXXXXXXXXXXXXXXXXXXXXXXXXXXXXXX
C
C    ROUTINE TO FIND THE WAVE LENGHT OF THE ELECTRON BEAM
C
C    CALLER PROGRAMS: ISPLIT,CHA,KAP,RDF
C
CXXXXXXXXXXXXXXXXXXXXXXXXXXXXXXXXXXXXXXXXXXXXXXXXXXXXXXXXXXXXXXXXXXXXX
C    SUBROUTINE MWLEN(ACCPOT,LAMBDA)
C    IMPLICIT REAL*8 (A-Z)
C    LSPEED=2.998E10      !SPEED OF LIGHT
C    RMASS=9.110E-28      !ELECTRON REST MASS
C    EV=1.602E-12         !EV CONVERSION
C    PLANK=6.626E-27      !PLANK'S CONSTANT
C
C    ENERGY=ACCPOT*EV
C    MOC2=RMASS*(LSPEED**2)
C    VELOC=LSPEED*DSQRT(1-(MOC2/(ENERGY+MOC2))**2)
C    BETHA=1.0/DSQRT(1-(VELOC/LSPEED)**2)
C    LAMBDA=PLANK/(BETHA*RMASS*VELOC)*1.0E8
C    RETURN
CXXXXXXXXXXXXXXXXXXXXXXXXXXXXXXXXXXXXXXXXXXXXXXXXXXXXXXXXXXXXXXXXXXXXX
C
C    ROUTINE SVAL
C
C    DETERMINES THE VALUE OF THE SCATTERING PARAMETER S AS A FUNCTION OF
C    THE POINT NUMBER
C
C    CALLER PROGRAMS:RDF,CHA,ISPLIT,FXIT,NORM
C
CXXXXXXXXXXXXXXXXXXXXXXXXXXXXXXXXXXXXXXXXXXXXXXXXXXXXXXXXXXXXXXXXXXXXX
C    FUNCTION SVAL(I)
C    IMPLICIT REAL*8 (A-H,O-Z)
C    REAL*8 LAMBDA
C    COMMON/BLOCK/LAMBDA,CAMK,DISINC
C    CAMK2=CAMK*CAMK
C    RR=(DISINC)*(1-I)      !DISTANCE THAT DENSITOMETER HAS
C                           !MOVED UP TO THE SPECIFIED POINT
C
C    RR2=RR*RR
C    TEMP1=CAMK/DSQRT(RR2+CAMK2) !FIND THE SINE OF ANGLE THAT
C    SINZHT=DSQRT(0.5*(1-TEMP1)) !CORRESPONDS TO THIS SMALLEST INTERVAL
C    SVAL=2.*(SINZHT)/(LAMBDA)  !FIND VALUE OF S
C    RETURN                  !RETURN
C    END

```

References

- 1) T.J. Chainer, D.A. Thompson and T.K. Worthington, Fall Meeting of the Electrochem. Soc., paper # 138
- 2) G.S. Cargill III, J. Appl. Phys., 41, 12 (1970)
- 3) T. Yamasaki, H. Izumi and H. Sunada, Scrip. Metall., 15, 177 (1981)
- 4) J.P. Marton, Ph.D. Thesis, University of Western Ontario
- 5) I. Kiflawi and M. Schlesinger, J. Electrochem. Soc., 130, 872 (1983)
- 6) J.L. Chow, N.E. Hedgecock, M. Schlesinger and J. Rezek, J. Electrochem. Soc., 119, 1614 (1972)
- 7) J.P. Marton and M. Schlesinger, J. Electroch. Soc., 115, 16 (1968)
- 8) E. Vafaei-Makhsoos, E.L. Thomas and L.E. Toth, Metall. Transc., 9A, 1449 (1978)
- 9) E. Vafaei-Makhsoos, J. Appl. Phys., 51, 12 (1981)
- 10) F. Zernike and J.A. Prins, Z. Phys., 41, 184 (1927)
- 11) P. Debye and H. Menke, Physikal. Zeit., 31, 797 (1930)
- 12) N.S. Gingrich, Rev. Mod. Phys., 15, 90 (1943)
- 13) J. Waser and V. Schomaker, Rev. Mod. Phys., 25, 671 (1953)
- 14) R. Hosemann and S.N. Bagchi, Direct Analysis of Diffraction by Matter, North Holland Publ.: Amsterdam 1962
- 15) A. Guinier, X-Ray Diffraction, Chapters 2 and 3, Freeman: San Francisco 1963
- 16) B.E. Warren, X-Ray Diffraction, Chapter 10, Addison-Wesley: Reading, Massachusetts 1969
- 17) D.B. Dove, Physics of Thin Films, Academic Press, Vol. 7, 1 (1973)

References

- 18) C.N.J. Wagner, Journal of Non-Crystalline Solids, **42**, 3 (1980)
- 19) M. Goldstein, Classical Mechanics, Addison-Wesley: Reading, Mass. 1956
- 20) J.D. Jackson, Classical Electrodynamics, 2nd edition, Wiley and Son: New York 1975
- 21) Watson, Theory of Bessel Functions 2nd edition, Cambridge 1952
- 22) N.F. Mott and H.S.W. Massey, the Theory of Atomic Collisions 3rd edition, Oxford University Press: New York 1965
- 23) see reference 22 page 89
- 24) P.A. Doyle and P.S. Turner, Acta Cryst., **A24**, 398 (1968)
- 25) reference 16, pages 121-122
- 26) G.S. Cargill III, J. Appl. Cryst., **4**, 277 1971
- 27) A. Savitzky and M.J.E. Golay, Anal. Chem., vol 36, No. 8, 1627 (1964)
- 28) T.H. James and G.C. Higgins, Fundamentals of Photographic Theory, John Willey & Son: London 1948
- 29) A. Papoulis, The Fourier Integral and its Applications, McGraw-Hill: New York 1962
- 30) E. Oran Brigham, The Fast Fourier Transform, Prentice-Hall: Englewood, New Jersey 1974
- 31) R.J. Bell, Introductory Fourier Transform Spectroscopy, Academic Press: New York 1972
- 32) R. Kaplow, S.L. Strong and B.L. Averbach, Phys. Rev., **138**, 1336 (1965)
- 33) J.F. Graczyk, P. Chaudhari, Phys. Stat. Soli. (b), **58**, 16

References

- (1973)
- 34) I. Kiflawi and M. Schlesinger, J. Electrochem. Soc., 130, 872 (1983)
- 35) B.E. Warren, J. Appl. Phys., 12, 375 (1941)
- 36) J.P. Marton and M. Schlesinger, J. Electrochem. Soc., 115, 16 (1968)
- 37) N. Feldstein, M. Schlesinger, N.E. Hedgecock and S.L. Chow, J. Electrochem. Soc., 121, 6 (1974)
- 38) M. Schelensiger and J.P. Marton, J. Appl. Phys., 40, 8 (1969)
- 39) J.W. Cooley and J.W. Tuckey, Math. Comp., 19, 297 (1965)
- 40) D.M. Monro, Appl. Statist., 24, 268 (1975)
- 41) D.M. Monro, Appl. Statist., 25, 166 (1976)

Vita Actoris

I was born in Madrid, Spain on July 7, 1958. At the tender age of six months my family moved to Sao Paulo, Brazil where we lived until 1965 at which time we returned to Madrid. In 1974 I came to Canada where I completed my high school education at Centennial S.S. In 1977 I enrolled in the University of Windsor where in 1981 I received a B.Sc. Honours Physics degree.